

Impact of stepwise NH₂-methylation of Triapine on the physico-chemical properties, anticancer activity and resistance circumvention

Christian R. Kowol,^{‡,§,≠,} Walter Miklos,^{#,≠} Sarah Pfaff,[‡] Sonja Hager,[#] Sebastian Kallus,[‡] Karla Pelivan,[‡] Mario Kubanik,[‡] Éva A. Enyedy,[†] Walter Berger,^{#,§} Petra Heffeter,^{#,§,*} Bernhard K. Keppler^{‡,§}*

[‡] Institute of Inorganic Chemistry, University of Vienna, Waehringer Str. 42, A-1090 Vienna, Austria

[#] Medical University of Vienna, Institute of Cancer Research, Borschkeg. 8a, A-1090 Vienna, Austria

[§] Research Platform “Translational Cancer Therapy Research” University of Vienna, Waehringer Str. 42, A-1090, Vienna, Austria

[†] Department of Inorganic and Analytical Chemistry, University of Szeged, Dóm tér 7, 6720 Szeged, Hungary

[≠] These authors contributed equally

***Authors for correspondence:** Institute of Inorganic Chemistry, University of Vienna, Waehringer Str. 42, A-1090 Vienna, Austria. Phone: +43-1-4277-52609. Fax: +43-1-4277-

52680. E-mail: christian.kowol@univie.ac.at.

Medical University of Vienna, Institute of Cancer Research, Borschkeg. 8a, A-1090 Vienna, Austria. Phone: +43-1-40160-57557. Fax: +43-1-40160-957555. E-mail: petra.heffeter@meduniwien.ac.at.

Abstract

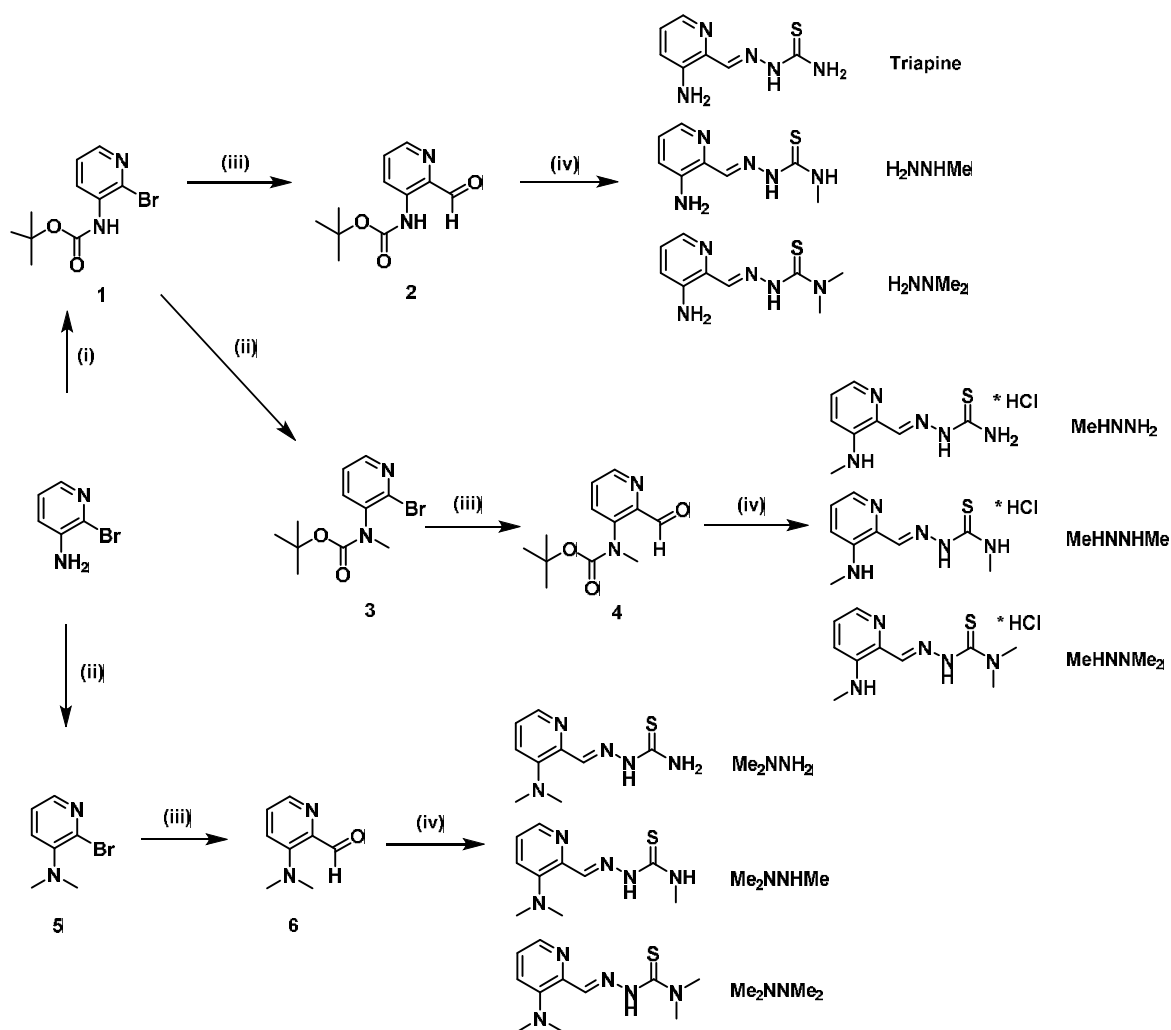
One of the most promising classes of iron chelators are α -*N*-heterocyclic thiosemicarbazones with Triapine as the most prominent representative. In several clinical trials Triapine showed anticancer activity against hematological diseases, however, studies on solid tumors failed due to widely unknown reasons. Some years ago, it was recognized that “terminal dimethylation” of thiosemicarbazones can lead to a more than 100-fold increased activity, probably due to interactions with cellular copper depots. To better understand the structural requirements for the switch to nanomolar cytotoxicity, we systematically synthesized all eight possible N-methylated derivatives of Triapine and investigated their potential against Triapine-sensitive as well as -resistant cell lines. While only the “completely” methylated compound exerted nanomolar activity, the data revealed that all compounds with at least one N-dimethylation were not affected by acquired Triapine resistance. In addition, these compounds were highly synergistic with copper treatment accompanied by induction of ROS and massive necrotic cell death.

Introduction

Due to the limited success of chemotherapeutic agents in the treatment of advanced cancer, novel anticancer drugs with different mechanisms of action need to be developed. One possibility is to target the deregulated iron metabolism of rapidly dividing cancer cells^{1, 2}. Therefore, several iron chelators have been developed. The first candidate with potential anticancer activity was desferrioxamine (DFO)², which entered clinical trials in the 1980s and showed remarkable results in leukemia³ as well as neuroblastoma patients⁴. Nevertheless, subsequent studies demonstrated failure of DFO as a potent anticancer agent^{5, 6} which was at least in part connected with the very short half-life time and low membrane permeability of this compound⁷. Consequently, numerous other iron chelating drugs have been developed to overcome these limitations^{2, 8}. One very promising class of iron chelators are α -*N*-heterocyclic thiosemicarbazones which harbor a *N,N,S* tridentate motif able to strongly coordinate to transition metal ions^{9, 10}. The most prominent and best characterized member is 3-aminopyridine-2-carboxaldehyde thiosemicarbazone, also known as 3-AP or Triapine⁷. Triapine is a highly efficient inhibitor of ribonucleotide reductase¹¹ (via destruction of the iron-dependent tyrosyl radical¹²), a crucial enzyme for the synthesis of dNTPs. In addition, also other thiosemicarbazones like di-2-pyridylketone 4,4-dimethyl-3-thiosemicarbazone (Dp44mt) and di-2-pyridylketone-4-cyclohexyl-4-methyl-3-thiosemicarbazone (DpC) are currently intensively investigated as drug candidates¹³. With regard to the clinical situation, Triapine showed promising anticancer activity in several clinical phase I and II trials on patients with hematological diseases^{14, 15}, while studies on solid tumors failed so far¹⁶⁻¹⁸. The reason for this lack of efficiency against solid tumors is currently not fully understood, but one hypothesis is rapid development of resistance. Therefore, our group has recently generated a Triapine-resistant colon carcinoma cell line to investigate the mechanisms underlying acquired Triapine resistance in solid cancer cells. Interestingly, very rapid up-

regulation of well-known multi-drug resistance mechanisms, such as ABCB1 (P-glycoprotein) and protein kinase C, were found, although Triapine is only a weak substrate for ATP-binding cassette transporters¹⁹.

In order to improve thiosemicarbazone-based therapy, in the last years multiple novel derivatives have been developed resulting in the discovery of several compounds with a distinctly increased cytotoxicity. One of these compounds was the α -pyridyl thiosemicarbazone Dp44mT which exhibited a more than 100-fold higher cytotoxicity than Triapine²⁰⁻²². This strongly increased activity was also shared by some other α -*N*-heterocyclic thiosemicarbazones published by our group and seems to be associated with the so-called “terminal dimethylation” (lack of hydrogen atoms at the terminal nitrogen atom)^{23, 24}. Interestingly, at least in case of Dp44mT, the improved anticancer activity was so far explained by interaction with cellular copper ions, which results in oxidative stress and apoptosis induction²⁵⁻²⁷. In order to fill the knowledge gap regarding the anticancer mechanisms of Triapine and the terminally dimethylated nanomolar cytotoxic derivatives, in this work, systematically all possible *N*-methylated derivatives of Triapine (Scheme 1) were synthesized and their physico-chemical as well as anticancer properties were analyzed. In particular, we focused on the detailed structure-activity relationship, mode of action studies and the impact of acquired Triapine resistance on the activity of the novel derivatives.



Scheme 1: Library of the investigated compounds. Reaction conditions: (i) (Boc)₂O, sodium bis(trimethylsilyl)amide; (ii) NaH, MeI; (iii) n-BuLi, DMF; (iv) respective thiosemicarbazide.

Results

Synthesis and characterization. The novel monomethylated 3-aminopyridine derivatives were synthesized by treatment of Boc-protected 3-amino-2-bromopyridine with methyl iodide in the presence of NaH. For dimethylation 3-amino-2-bromopyridine was directly treated with excess methyl iodide/NaH. Subsequently, in both cases, the bromo species were converted to the

respective aldehydes using *n*-butyllithium (*n*-BuLi) and dimethylformamide (DMF), which were finally reacted with the respective thiosemicarbazides (Scheme 1). For the monomethylated 3-aminopyridine derivatives, in the last step, conc. HCl was added for deprotection resulting in formation of the HCl salts (Scheme 1).

The ¹H-NMR spectra of the **H₂NNR₂** series in dimethylsulfoxide (DMSO)-*d*₆ showed only one isomeric form with the N-NH signal around 11.1–11.4 ppm. This indicates the presence of the so-called *E*-isomer of 2-formylpyridine thiosemicarbazones²⁸. Also the HCl-salts of the **MeHNRR₂** series resonated in this region (11.8–12.2). In contrast, for all three **Me₂NNR₂** derivatives two sets of signals could be observed in DMSO-*d*₆: the *E*-isomer again in the region 11.1–11.6 ppm and a second N-NH signal between 13.9–15.2 ppm attributed to the *Z*-isomer. This strong low field shift can be explained by the involvement of the N-NH moiety in an intramolecular hydrogen bond. This bond also strongly influences the shift of the HC=N proton (*E*-isomer: ~8.5, *Z*-isomer: ~7.5) and the corresponding carbon C=N signal (*E*-isomer: ~142 ppm, *Z*-isomer: ~132 ppm). Noteworthy, in case of **Me₂NNH₂** and **Me₂NNHMe**, the unpurified spectra showed both isomers, whereas after chromatographic purification only the pure *E*-isomer was present. In contrast, for **Me₂NNMe₂** both isomers were observed in the NMR spectrum after column chromatography.

X-ray quality crystals of **Me₂NNH₂** were obtained from a water solution stored at 4°C. Results of X-ray diffraction analysis are shown in Figure 1A, together with selected bond lengths and angles. **Me₂NNH₂** crystallized in the monoclinic space group P2₁/c and adopts the *Z*-isomeric form, with a hydrogen bond between N1 and N4, in contrast to Triapine with *E*-configuration²³.

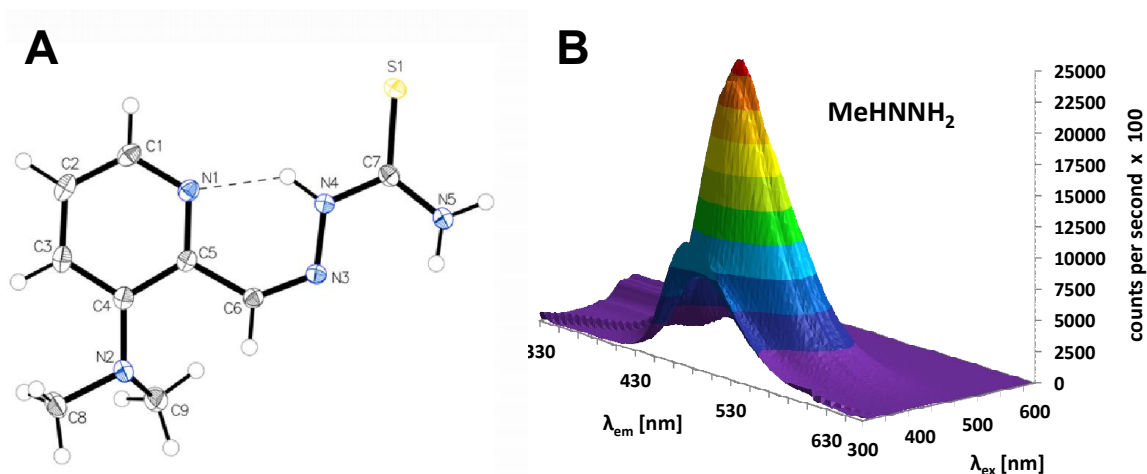


Figure 1: A) X-ray crystal structure of **Me₂NNH₂**. The thermal ellipsoids are drawn at 50% probability levels. Selected bond lengths (Å) and angles (deg): C6–N3 1.2957(15), N3–N4 1.3649(14), N4–C7 1.3526(15), C7–S1 1.6850(12), C7–N5 1.3272(16) Å; $\Theta_{(N2-C4-C5-C6)}$ – 5.88(17), $\Theta_{(C5-C6-N3-N4)}$ –0.84(18), $\Theta_{(N3-N4-C7-S1)}$ 177.52(8)°. B) 3D fluorescence spectrum of **MeHNNH₂** in 1% DMSO/PBS (10 μM) at pH 7.4.

Due to the intrinsic fluorescence properties of Triapine,²⁹ the series of new derivatives was also investigated by fluorescence spectroscopy (conditions: 10 μM in 1% DMSO/phosphate buffered saline (PBS), pH 7.4). Maximum of the excitation wavelength, emission wavelength and intensity of emitted fluorescence light are listed in Table 1 and a 3D fluorescence plot of **MeHNNH₂** is shown in Figure 1B. Concerning the fluorescence intensity, no general trends could be observed, only the **Me₂NNR₂** series showed distinctly lower intensity compared to the other derivatives. The maxima of the excitation wavelengths correlate as expected with the highest bands at the highest λ_{max} in the UV/vis spectra. Noteworthy, the excitation maximum increases from the **H₂NNR₂** series at ~370 nm to the **MeHNNR₂** derivatives at ~400 nm. However, unexpectedly it strongly decreases to ~350 nm in the three **Me₂NNR₂** compounds.

Table 1: Fluorescence data of Triapine and its derivatives

Compound^a	Excitation maximum /nm	Emission maximum /nm	Counts per second^b
Triapine	368	454	1,360,000
H₂NNHMe	364	448	1,109,300
H₂NNMe₂	368	422	1,530,600
MeHNNH₂	396	482	2,360,200
MeHNNHMe	392	482	1,524,900
MeHNNMe₂	396	492	378,600
Me₂NNH₂	352	506	409,200
Me₂NNHMe	352	500	731,300
Me₂NNMe₂	352	482	670,700

^aDMSO stock solutions of all compounds were diluted with PBS (pH 7.4) to a final concentration of 10 μ M (1% DMSO); ^b Measured at the maxima of the excitation and emission wavelengths.

The lipo-hydrophilic character of the compounds was studied at pH 7.4 via partitioning between *n*-octanol and water (Table 2). According to the pK_a values of Triapine and H₂NNMe₂, both are neutral (100% HL) at pH 7.4³⁰, which can also be expected for the other derivatives. Thus, the $\log D_{7.4}$ values are considered to be equal to the $\log P$ values of the compounds.

Table 2: Log $D_{7.4}$ values (*n*-octanol/water) for the Triapine derivatives [25 °C, pH = 7.40, 10 mM 4-(2-hydroxyethyl)-1-piperazineethanesulfonic acid (HEPES) and $I = 0.10$ M (KCl)].

	λ_{\max} / nm (water)	λ_{\max} / nm (<i>n</i> -octanol)	logD_{7.4}	SD	log P predicted with Chemdraw
Triapine	360	376	0.85 ^a	-	-0.02
H₂NNHMe	360	372	1.20	0.03	0.50
H₂NNMe₂	362	374	1.30 ^b	-	0.88
MeHNNH₂	386	396	1.40	0.10	0.28
MeHNNHMe	384	392	2.03	0.10	0.80
MeHNNMe₂	386	394	2.10	0.01	1.18
Me₂NNH₂	348	364	1.21	0.02	1.07
Me₂NNHMe	350	364	1.86	0.01	1.59
Me₂NNMe₂	352	372	1.52	0.03	1.97

^a Value is taken from Ref [³⁰]; ^b Value is taken from Ref [³¹]

Stepwise methylation of Triapine up to **MeHNNMe₂** as expected increased the lipophilicity. Noteworthy, the methylation of NH₂ → NHMe had a much stronger influence on the lipophilicity compared to the NHMe → NMe₂ step. However, again trends of the **Me₂NNR₂** derivatives did not correlate with all other compounds. Unexpectedly, the logD_{7.4} values were below that of the **MeHNNR₂** series and, in addition, there was no stepwise increase from terminal NH₂ to NMe₂. In general, the obtained logD_{7.4}/P values were much higher than the values predicted with

ChemDraw software. This once again confirms that the calculation of logP values is often afflicted with errors (especially when isomerization or intermolecular bonding is non-considered).

Synthesis and investigation of isomers. The fact that the physico-chemical parameters (UV/vis and fluorescence maxima, lipophilicity) of the three derivatives of the **Me₂NNR₂** series did not fit into the expected range, prompted us to further investigate this set of compounds. As the NMR spectra of the **Me₂NNH₂** series already indicated the presence of two isomers (in contrast to the other six compounds), we aimed to isolate both isomers as pure compounds. In case of **Me₂NNH₂** and **Me₂NNHMe**, the standard synthesis with chromatographic purification already yielded the pure E isomers. To obtain the respective Z isomers, the E isomers were stirred in acetonitrile for 24 h at 37°C. This was necessary because solvents with a low donor number³² were previously reported to stabilize the Z isomer^{28, 33}. Indeed, this approach resulted in partial conversion of the two compounds and allowed isolation of the pure Z isomers of **Me₂NNH₂** and **Me₂NNHMe** after chromatographic separation. For **Me₂NNHMe₂**, the isomers could not be separated due to a very fast interconversion.

As next step, the isomerization process of all nine compounds including the purified E and Z isomers of **Me₂NNH₂** and **Me₂NNHMe** were studied in PBS at pH 7.4 via high-performance liquid chromatography (HPLC) coupled to a mass spectrometry (MS) detector (Table 3).

Table 3: Isomerization study in PBS at pH 7.4 via HPLC-MS.^a

Compound	0 h		24 h	
	% Isomer 1	% Isomer 2	% Isomer 1	% Isomer 2
Triapine	100 (7.7) ^b	-	100	-
H ₂ NNHMe	100 (10.0)	-	100	-
H ₂ NNMe ₂	100 (10.2)	-	100	-
MeHNNH ₂	100 (10.5)	-	100	-
MeHNNHMe	99 (11.3)	1 (9.8) ^b	99	1
MeHNNMe ₂	98 (11.3)	2 (10.3)	98	2
(<i>E</i>)-Me ₂ NNH ₂	-	100 (10.3)	8	92
(<i>Z</i>)-Me ₂ NNH ₂	94 (13.9)	6 (10.3)	6	94
(<i>E</i>)-Me ₂ NNHMe	4 (16.3)	96 (11.1)	15	85
(<i>Z</i>)-Me ₂ NNHMe	93 (16.3)	7 (11.1)	13	87
Me ₂ NNMe ₂	c	c	c	c

^a DMSO stock solutions of all compounds were diluted with PBS (pH 7.4) to a final concentration of 50 μ M (1% DMSO) and immediately measured by HPLC-MS. All measured values are $\pm 2\%$. ^b The numbers in brackets correspond to the HPLC-MS retention time (min) of the compounds. ^c In case of Me₂NNMe₂, only one very broad peak was obtained, which was not possible to be separated into the two isomers, presumably due to the fast interconversion on the column.

In aqueous solution, the N-NH protons, which are usually used for the assignment of E and Z isomer in organic solvents via NMR spectroscopy, are not detectable anymore. Thus, for the HPLC measurements, the respective retention times were used as assignment parameters (the different isomers were termed isomer 1 and 2). The measurements performed directly after dissolution in PBS showed a clear increase of the retention times with increasing number of methyl groups. Consequently, Triapine was found at 7.7 min, followed by **MeHNNMe₂** at 11.3 min, **(Z)-Me₂NNH₂** at 13.9 min and finally **(Z)-Me₂NNHMe** at 16.3 min. For **Me₂NNMe₂** only a very broad peak was observed, presumably due to fast interconversion of the isomers on the column. In contrast, the synthesized E-isomers are not in line with this trend, with **(E)-Me₂NNH₂** at 10.3 min and **(E)-Me₂NNHMe** at 11.1 min. After 24 h the isomeric pattern was identical for all derivatives, except for the purified E and Z isomers of **Me₂NNH₂** and **Me₂NNHMe**, which interconverted and reached an equilibrium with ~90% isomer 2 and 10% isomer 1 (Figure 2). In contrast to all other derivatives, in case of **Me₂NNH₂** and **Me₂NNHMe**, the isomer 2 was stabilized in PBS solution. This could explain why the measured UV/vis and fluorescence maxima as well as lipophilicity do not follow a clear trend within all nine compounds.

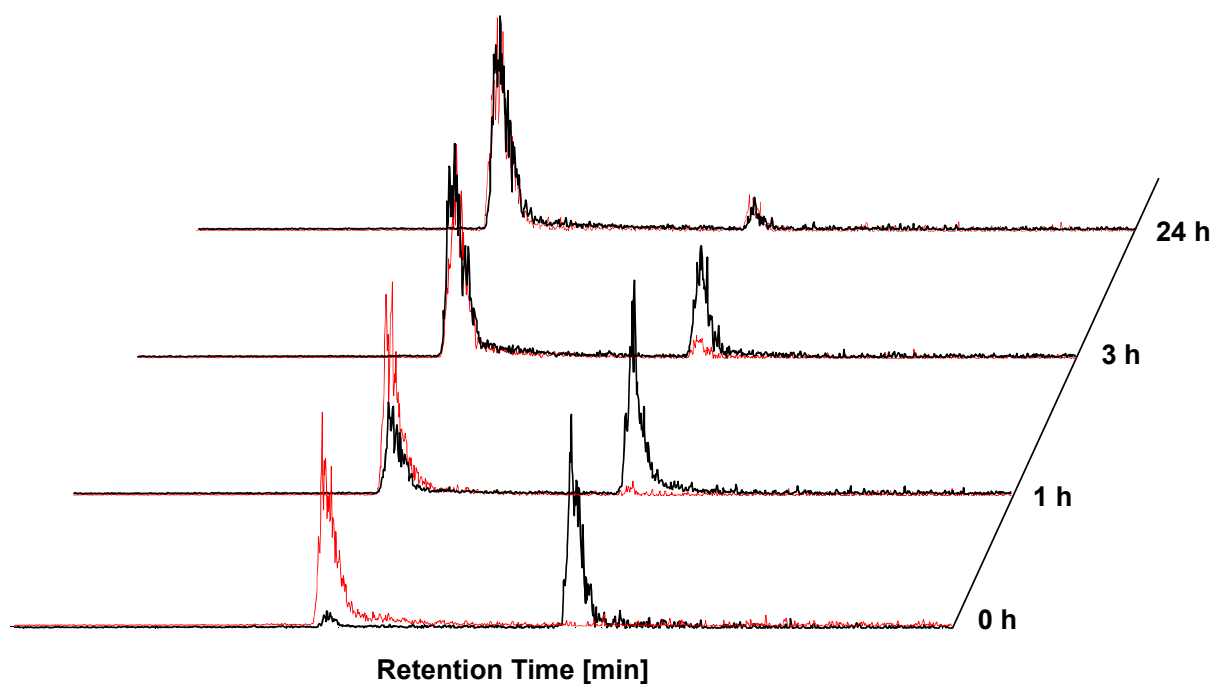


Figure 2: Interconversion of isomer 1 (black) and isomer 2 (red) of Me_2NNH_2 in PBS at pH 7.4.

Cytotoxicity. To assess the impact of the structural modifications in the Triapine backbone on the antitumor activity, Triapine and its eight derivatives were tested against the colon adenocarcinoma SW480, the ovarian carcinoma A2780, selected Triapine-resistant SW480/Tria cells¹⁹, the cervix carcinoma KB-3-1 together with its ABCB1-overexpressing subline KBC-1, and finally the lung fibroblast line Wi38. To this end, 3-(4,5-dimethylthiazol-2-yl)-2,5-diphenyltetrazolium bromide (MTT) assays were performed after 72 h of drug incubation.

In the cancer cell model, all compounds revealed IC_{50} values in the low μM range with rather minor differences (Table 4). The only remarkable exception was Me_2NNMe_2 , exerting extremely increased activity with IC_{50} values in the low nM range. With regard to the structural differences, in the chemosensitive A2780 and SW480, terminal monomethylation in case of H_2NNHMe and

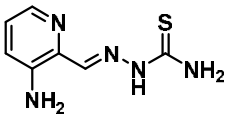
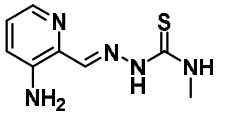
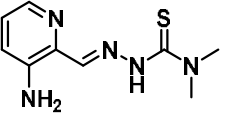
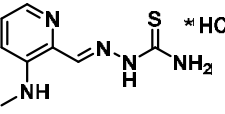
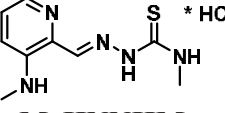
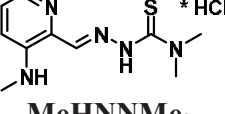
MeHNNHMe resulted in decreased activity (e.g. in SW480 cells by 2.9- and 2.3-fold, respectively) compared to the terminal NH₂ derivatives. In contrast, terminal dimethylation showed a tendency to increase the cytotoxicity in case of **H₂NNMe₂** and **MeHNNMe₂**. Also monomethylation of the pyridine NH₂ slightly decreased the anticancer activity in both cells lines compared to the non-methylated derivatives. Notably, dimethylation of the pyridine NH₂ resulted in strong variances between the individual experiments, indicated by the rather high standard deviations of the respective IC₅₀ values. Interestingly, these are exactly the derivatives where the presence of different isomers was observed (in case of **Me₂NNH₂** and **Me₂NNMeH**, both the isomeric mixture and the pure E and Z isomers were tested, however, without significant differences). Furthermore, clearly diminished activity of **Me₂NNH₂** compared to Triapine as well as a dramatic increase from **H₂NNMe₂** to **Me₂NNMe₂** (43-fold in A2780 cells) was found, resulting in nanomolar activity for **Me₂NNMe₂**.

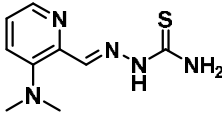
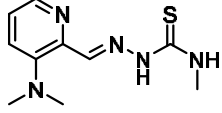
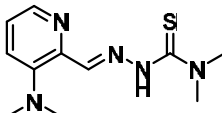
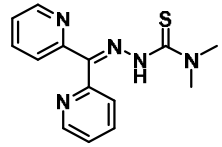
Interestingly, Triapine-resistant SW480/Tria cells responded differently as compared to the parental SW480 cells. In general, with increasing number of methylation sites also the cytotoxicity increased regardless whether methylation was at the pyridine NH₂ or at the terminal NH₂ position. Hence, the observed order of activity was **Triapine** < **H₂NNHMe** < **H₂NNMe₂** and **Triapine** < **MeHNNH₂** < **Me₂NNH₂**. **Me₂NNMe₂** again was the most active thiosemicarbazone, with IC₅₀ values in the nM range. Also the degree of resistance (resistance factor is shown in Table 4) markedly decreased with increased methylation of the pyridine NH₂ and terminal NH₂ groups. Thus, SW480/Tria cells were highly cross-resistant against Triapine derivatives with one methyl group (**H₂NNHMe** and **MeHNNH₂**). For **MeHNNHMe**, the activity was not diminished in the Triapine-resistant cell model. In contrast, for all thiosemicarbazones, with at least one NMe₂ moiety, the activity was even higher in the Triapine-resistant cell line compared to the parental SW480 cells (in most cases the IC₅₀ levels were about ~0.5-fold compared to the

parental cells). However, due to the high standard deviation of the derivatives with dimethylation of the pyridine NH₂, only **MeHNNMe₂** reached statistical significance). This clearly indicates that dimethylation of one of the two amino groups is able to efficiently overcome acquired Triapine resistance or even induce a tendency towards collateral sensitivity. To investigate also the contribution of ABCB1 expression on the activity, our test panel was additionally tested on KB-3-1 cells in comparison to its highly ABCB1-overexpressing subline KBC-1. In agreement to our previous publication¹⁹, KBC-1 displayed a weak (2.9-fold) resistance to Triapine and closely related derivatives like **H₂NNHMe**, **MeHNNH₂**, **MeHNNHMe**, whereas drug resistance was reduced (not significant) by terminal dimethylation. However, dimethylation at the pyridine NH₂ in case of **Me₂NNH₂** and **Me₂NNHMe** induced significant collateral sensitivity of KBC-1 cells.

Finally, the impact of our test panel on non-malignant lung fibroblasts (WI38) was investigated. Overall, this cell line was in general less sensitive towards our compound panel than the cancer cell lines, especially A2780. However, it might be worth noting that the structure-activity relationship of WI-38 differed to some extent from the cancer cell models. Such, it displayed the highest sensitivity towards all compounds harboring a terminal dimethylation (**H₂NNMe₂**, **MeHNNMe₂**, **Me₂HNNMe₂**), with IC₅₀ values ~1 μM. This also implies that **Me₂NNMe₂** showed no nanomolar activity in this cell model. Overall, these data indicate a cancer cell-specific activity window for several compounds of our panel including **Me₂HNNMe₂**. This is also supported by preliminary toxicity tests of **Me₂NNMe₂** in mice revealing no differences in the tolerability compared to e.g. Triapine.

Table 4: IC₅₀ values (μM) of Triapine and its derivatives in different cancer cell lines after 72 h drug treatment.

Compound	A2780	SW480	SW480/Tria (resistance factor)	KB-3-1	KBC-1 (resistance factor)	WI-38
 Triapine	0.7 ± 0.3	0.84 ± 0.25	> 50 (>60) ^{***}	3.1 ± 1.2	8.9 ± 0.4 (2.9) ^{***}	> 25
 H₂NNHMe	0.9 ± 0.1	2.51 ± 0.58	9.5 ± 0.7 (3.8) ^{***}	4.7 ± 1.2	20.9 ± 1.3 (4.4) ^{***}	> 25
 H₂NNMe₂	0.30 ± 0.03	0.52 ± 0.25	0.3 ± 0.1 (0.6) ^{n.s.}	0.79 ± 0.08	1.4 ± 0.8 (1.8) ^{n.s.}	1.1 ± 0.8
 MeHNNH₂	0.6 ± 0.2	1.37 ± 0.54	10.0 ± 0.04 (7.3) ^{***}	2.3 ± 0.6	10.3 ± 2.2 (4.5) ^{**}	11.3 ± 1.9
 MeHNNHMe	1.1 ± 0.3	3.16 ± 0.80	4.6 ± 0.6 (1.5) [*]	4.4 ± 0.3	9.5 ± 2.7 (2.2) [*]	9.2 ± 0.4
 MeHNNMe₂	0.40 ± 0.03	1.36 ± 0.98	0.30 ± 0.06 (0.2) [*]	4.2 ± 0.3	3.1 ± 0.8 (0.7) ^{n.s.}	1.7 ± 0.7

 Me₂NNH₂	6.4 ± 1.1	5.97 ± 3.02	4.8 ± 3.6 (0.8) ^{n.s.}	>50	14.6 ± 6.2 (<0.3) ^{***}	11.2 ± 4.2
 Me₂NNHMe	0.9 ± 0.2	5.98 ± 3.06	2.9 ± 0.7 (0.5) ^{n.s.}	>50	7.2 ± 4.2 (<0.2) ^{***}	5.2 ± 1.2
 Me₂NNMe₂	0.0070 ± 0.0003	0.05 ± 0.02	0.03 ± 0.02 (0.6) ^{n.s.}	0.06 ± 0.02	0.041 ± 0.004 (0.68) ^{n.s.}	1.0 ± 0.9
 Dp44mT	n.t.	0.06 ± 0.01	0.2 ± 0.1	0.070 ± 0.008	n.t.	0.4 ± 0.5

*** $p \leq 0.001$, ** $p \leq 0.01$, * $p \leq 0.05$, ^{n.s.} not significantly different, calculated by student's T test with

Welch's correction

Despite their similarities in IC₅₀ values (except **Me₂NNMe₂**), the morphological evaluations of the treated cells revealed distinct differences between the tested derivatives (exemplary images taken after 48 h incubation time are shown in Figure 3A). In general, the tested substance panel could be divided into two categories based on the induction of characteristic morphologic phenotypes: 1) induction of massive cell flattening resulting in distinctly increased cell size and surface area (especially pronounced for **Triapine**, **H₂NNHMe**, and **MeHNNH₂**), in contrast to 2) mild cell flattening accompanied by appearance of vesicular blebbing in the cytosol (Figure 3B; especially pronounced for **MeHNNMe₂**, **Me₂NNHMe**, and the nanomolar cytotoxic **Me₂NNMe₂**). Based on already available data for the nanomolar derivative Dp44mT^{27,13,34}, this

could indicate a structure-dependently increasing impact of the compounds on lysosomal compartments.

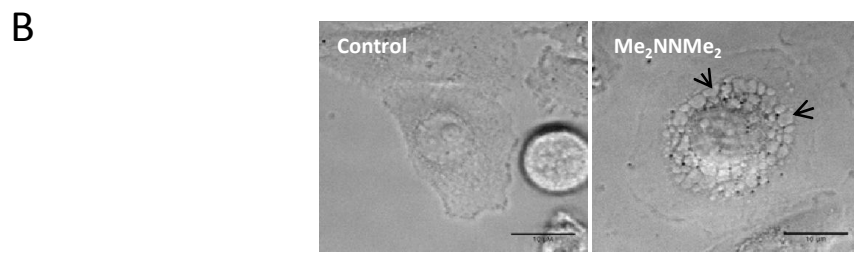
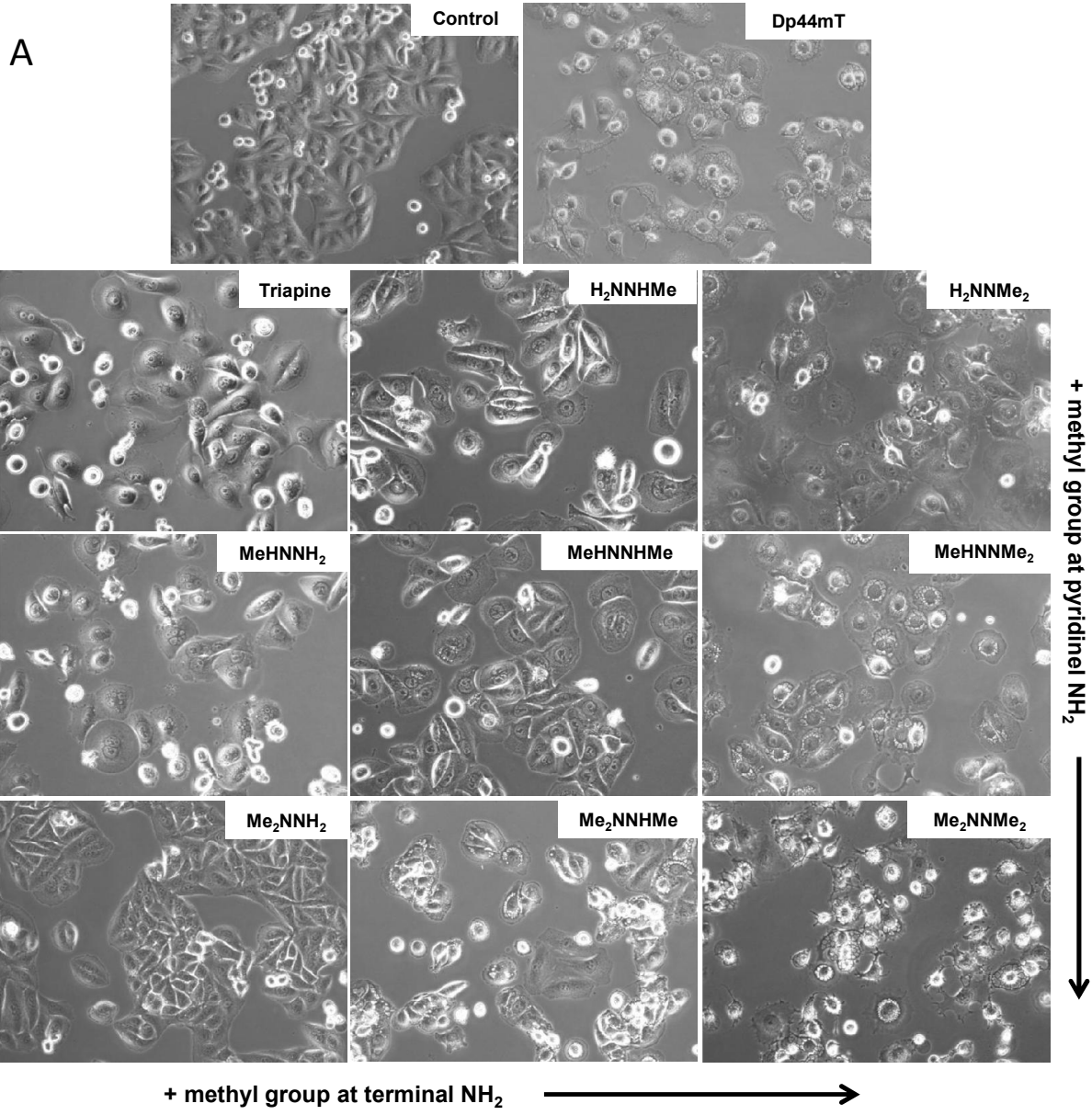


Figure 3: **A)** Phase contrast images of SW480 cells treated with 2.5 μM of the indicated drugs for 48 h (200 x-magnification). **B)** Vacuoles in SW480 cells induced by 24 h treatment of **Me₂NNMe₂** shown at 400 x-magnification. At early time points, vacuolization was predominantly perinuclear, but eventually the vacuoles fill the entire cytoplasmic space. Scale bar: 10 μm .

Recently, Ishiguro et al. showed that Triapine differs from the terminally dimethylated nanomolar cytotoxic Dp44mT and P44mT (pyridine-2-carboxaldehyde 4,4-dimethyl-3-thiosemicarbazone) in its interaction with copper ions.²⁵ Thus, we investigated the impact of pre-incubation with CuCl_2 on the activity of our thiosemicarbazone panel (Figure 4). In agreement with the published data, CuCl_2 (when given in excess or at least in a 1:1 ratio) had potent protective effects towards Triapine. In contrast, the nanomolar derivative **Me₂NNMe₂** was highly synergistic with CuCl_2 (with combination indices (CI values) down to 0.02, Supporting Information Figure S1), which is in line with the data on the nanomolar Dp44mT (Figure S2) and P44mT.²⁵ In addition, strong synergism with CuCl_2 was also observed for **MeHNNMe₂**, **Me₂NNH₂**, **Me₂NNHMe** and at higher concentrations with **H₂NNMe₂** and **MeHNNHMe** (the strongest effects were observed for **MeHNNMe₂** where CI values below 0.0001 were calculated, Figure S1). 2',7'-Dichlorofluorescein diacetate (DCF-DA) staining experiments suggested that this higher cytotoxic activity in the presence of CuCl_2 is associated with induction of reactive oxygen species (ROS; Figure 5A). As higher drug concentrations of **Me₂NNHMe** and **Me₂NNMe₂** (5 μM drug with 10 μM CuCl_2) decreased the DCF-DA signals to the level of untreated cells, tests for membrane integrity using the fluorescent dye propidium iodide (PI) were performed. These indicated that at the given conditions massive necrotic cell death (~80% of the cells were found

to be PI-positive) occurred (Figure 5B). Consequently, the lack of DCF-DA signal in these cells might be explained by enhanced membrane permeability (due to treatment-induced ROS) and consequently, reduced retention of DCF inside the cells.

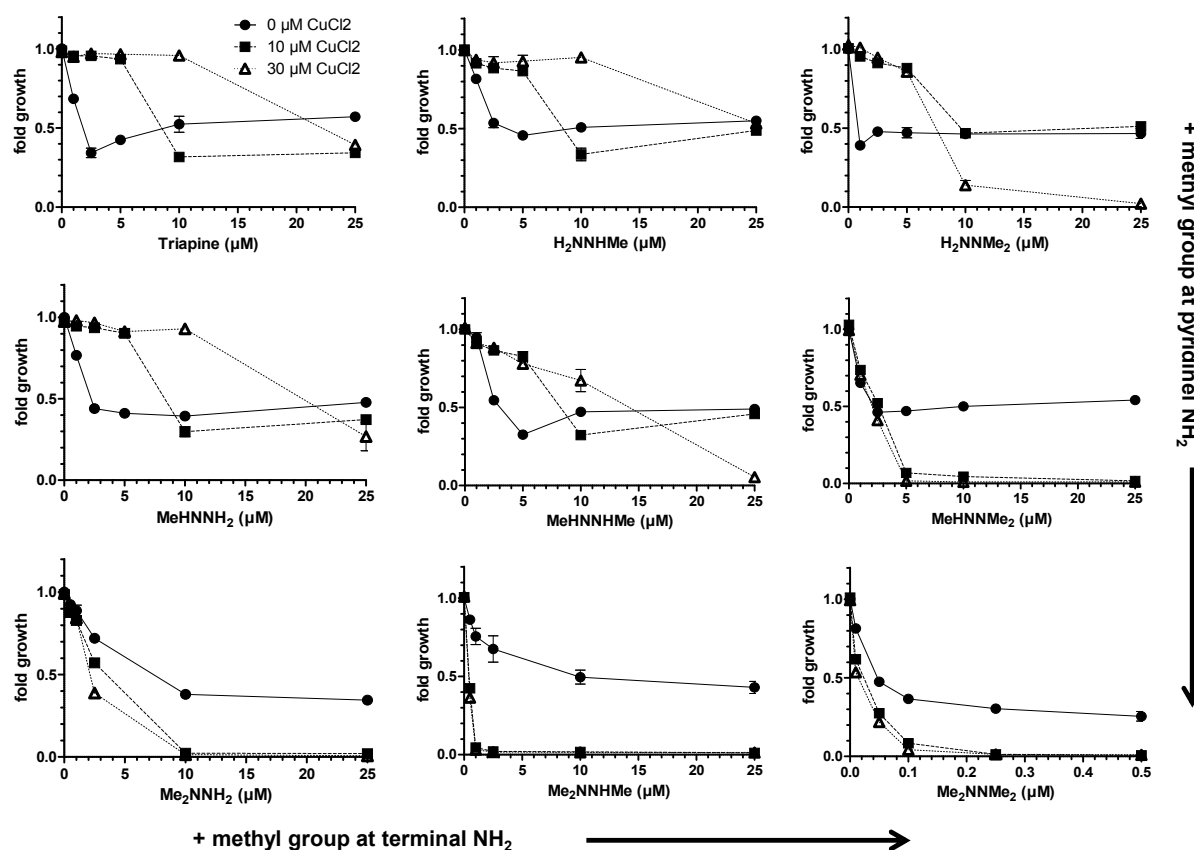


Figure 4: Impact of structural modifications of Triapine on the cytotoxicity in the presence of Cu(II) ions. Briefly, after 60 min pre-incubation with CuCl₂ (10 and 30 μM), SW480 cells were treated for 72 h with the indicated concentrations of Triapine and its derivatives. Viability was determined using MTT assay. The values given are the mean ± the standard deviation of triplicates from one representative experiment out of three.

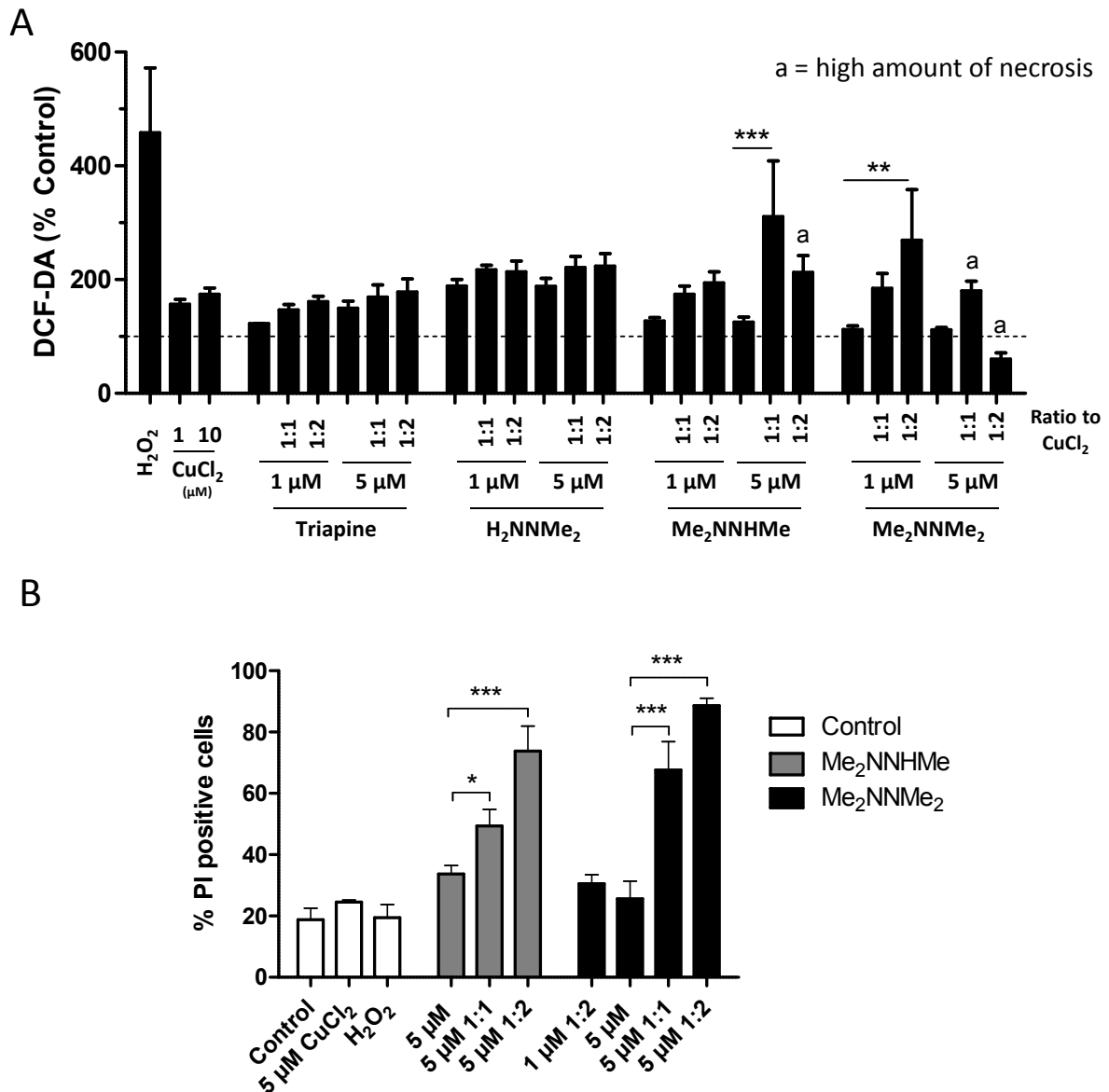


Figure 5: A) Intracellular ROS production in HL-60 cells after 30 min treatment of Triapine or its derivatives and prior 15 min incubation with CuCl₂. As positive control, H₂O₂ was used. DCF-DA fluorescence was measured using flow cytometry. B) Percentage of dead cells in conditions according to the DCF-DA assay. Cells were stained with Hoechst/PI and the percentage of PI-positive cells was determined microscopically. 1:1 and 1:2 is the ligand to copper(II) ion ratio. The values given are the mean ± the standard deviation of three experiments. Significances were

established using one-way ANOVA with Bonferroni's multiple comparison test (***) $p \leq 0.001$; ** $p \leq 0.01$, * $p \leq 0.05$).

Discussion and Conclusion

Thiosemicarbazones are known for their promising biological activity, which resulted in their clinical development as anticancer drugs. The best investigated agents of this class of compounds are Triapine and Dp44mT^{7, 8,35}. Noteworthy, Triapine has been tested in multiple clinical trials, showing promising activity in hematological diseases^{13, 14}. However, there is so far no proof of anticancer activity of Triapine when given as mono-treatment against solid tumors³⁶. The reasons for this are widely unexplored and make the development of novel thiosemicarbazone-based drugs interesting. Dp44mT has been well studied in multiple preclinical studies, indicating that this compound strongly differs from Triapine in several aspects. For example, Dp44mT was characterized by a distinctly higher ($IC_{50} \sim nM$) anticancer activity and a very high affinity for copper(II) ions^{26,13,27}. Also some of the thiosemicarbazone derivatives developed from our group shared this shift of activity to the nM range²³. Our data indicated that this pronounced anticancer activity is associated with terminal nitrogen dimethylation but only in the absence of any NH_2 functionality in the thiosemicarbazone backbone. Noteworthy, this increased activity was not accompanied by a similar increase in ribonucleotide reductase inhibition²³.

In the here presented study, the structure-activity relationship of Triapine derivatives was investigated in detail using the complete panel of stepwise methylated Triapine analogues. Our new panel was synthesized with the aim to allow detailed structure-activity/mode of action studies as well as development of novel derivatives to overcome Triapine resistance. Overall, several (rather unexpected) conclusions can be drawn from our results: 1) in contrast to the expected correlation of increased methylation of Triapine with changes in physico-chemical

properties, the **Me₂NNR₂** series showed unexpected behavior in terms of lipophilicity and characteristics of the UV/vis spectra. Subsequent studies revealed that this is based on isomerization and stabilization of a different isomer in buffered aqueous solution. Therefore, simple prediction of physico-chemical properties does not seem to be possible for this class of compounds. 2) The shift of the cytotoxic activity to the nanomolar range was only observed for one derivative namely: **Me₂NNMe₂**. This means that already the presence of only one hydrogen atom either at the terminal nitrogen or at the aminopyridine nitrogen distinctly reduced the anticancer potential of the drug by ~100–1000-fold. This is in contrast to some reports on several Richardson-type dipyridyl complexes, which did not follow this structure activity relationship when tested on SK-N-MC neuroepithelioma cells^{22, 37}. In detail, in this cell line several of Richardson's complexes with terminal NHR-moiety (R = methyl, ethyl, phenyl or allyl) were of similar activity like the terminally dimethylated Dp44mT. However, a study of the same complexes in 28 different cell lines revealed an average IC₅₀ value of 0.03±0.01 μM for Dp44mT, whereas the four thiosemicarbazones with terminal NHR had average IC₅₀ values of 0.20–1.70 μM²¹. Thus, these average cytotoxicity data followed the trend of our study with distinctly increased activity of compounds without any NH group. Noteworthy, these data also suggest that the activity enhancement by complete dimethylation is cell context-dependent, which is in agreement with our data revealing much stronger differences in case of A2780 compared to SW480 cells. 3) The impact of Triapine resistance on the activity of the novel derivatives was strongly associated with methylation of the pyridine and terminal NH₂ group. SW480/Tria cells were cross-resistant or equally active to compounds with only mono-methylation of one or both NH₂-groups (**H₂NNHMe**, **MeHNNH₂** and **MeHNNHMe**). In contrast, all compounds with at least one NH₂-dimethylation were not affected by the Triapine-resistance of SW480/tria. This clearly indicates that dimethylation of one of the two amino groups is a valuable tool to

efficiently overcome acquired Triapine resistance and suggests a different mode of action. Furthermore, it shows that the nanomolar activity is not mandatory for circumventing Triapine resistance. 4) Preliminary studies using ABCB1-overexpressing cells indicate that the impact of this efflux pump differs within the Triapine derivatives. Such, in agreement to our previous publication¹⁹, KBC-1 displayed a weak resistance to Triapine and closely related derivatives like **H₂NNHMe**, **MeHNNH₂**, **MeHNNHMe**. In contrast, drug resistance was reduced (not significant) by terminal dimethylation. Dimethylation at the pyridine NH₂ in case of **Me₂NNH₂** and **Me₂NNHMe** induced significant collateral sensitivity of KBC-1 cells. The nanomolar **Me₂NNMe₂** showed no significant differences between KB-3-1 and KBC-1. This is in contrast to data on Dp44mT, where induction of collateral sensitivity was recently published in KBV-1 cells^{34, 35} and might indicate some differences between Dp44mT and our nanomolar compound. 5) The observed hyper-activity on Triapine-resistant cancer cells positively correlated with the appearance of vesicular blebbing. This is a first hint on the molecular differences between classical thiosemicarbazone like Triapine and novel derivatives especially those with three and four methyl groups (**MeHNNMe₂**, **Me₂NNHMe** as well as the nanomolar **Me₂NNMe₂**) which are able to circumvent Triapine resistance. 6) Also with respect to the interaction with copper(II) ions, distinct differences were observed in our study. Thus, compounds which are inefficient against SW480/Tria cells, also showed reduced cytotoxicity in the presence of copper(II) ions. In contrast, hyperactive compounds (again especially **MeHNNMe₂**, **Me₂NNHMe**, and the nanomolar **Me₂NNMe₂**) were highly synergistic with copper(II) treatment accompanied by induction of ROS and massive necrotic cell death. In general, ROS production by **Me₂NNMe₂** is not surprising, as it is in good agreement with data on Dp44mT, reporting copper-dependent ROS production by this thiosemicarbazone with nanomolar cytotoxicity^{25, 27}. However, our data indicate that the increased cytotoxicity in the presence of copper(II) ions is not the (only) reason

for the nanomolar activity of some thiosemicarbazones, as also **MeHNNMe₂** and **Me₂NNHMe** with a low micromolar cytotoxicity show this synergistic effect. Noteworthy, the reasons underlying this very specific interaction with copper ions are still not fully understood. Ishiguro et al., for example, suggested that copper(II) complexes of Triapine and, in general, thiosemicarbazones without terminal dimethylation are able to get desulfurized in aqueous basic media with formation of insoluble CuS²⁵. However, as already indicated by Ishiguro et al., our previous solution equilibrium studies on Triapine and several related derivatives, did not show any indications for such an irreversible process. In contrast, Lovejoy et al. suggested that due to its “polyprotic nature”, Dp44mT is specifically trapped in the acidic lysosomes after protonation of the first pyridyl moiety and subsequent copper binding by the second resulting in formation of a positively charged copper complex²⁷. Noteworthy, despite several similarities to Dp44mT, all our derivatives contain only one pyridyl group. Consequently, the mechanisms suggested for cytotoxic activity of Dp44mT cannot explain the differences observed with regard to the interaction with copper in our study. Solution equilibrium studies showed that terminal dimethylation of thiosemicarbazones significantly increased the copper(II) binding abilities compared to derivatives with a terminal NH₂ moiety³⁸. However, already the stability of the copper(II) complex in case of Triapine is outstandingly high with >99% [CuL]⁺ at 1 μM at pH 7.4. Thus, also the stability does not seem to be the crucial parameter and probably other factors like the thermodynamics and kinetics of the reduction process in the cellular environment are important. These studies are currently in progress in our group. Nevertheless, the rapid necrotic cell death observed with some derivatives in the presence of copper should be also considered carefully with respect to a possible application in vivo. Especially as it is well known that induction of necrosis can result in inflammatory reactions of the body³⁹. Moreover, it has to be considered that various cancer types are frequently associated high serum copper levels^{40, 41}

Consequently, treatment of such patients with copper-synergizing thiosemicarbazones might be associated with increased occurrence of adverse effects due to ROS production.

Summarizing, we systematically synthesized a panel of N-methylated Triapine derivatives and investigated their biological modes of action. Our data gave new insights into the coherences between methylation, cross-resistance to Triapine, nanomolar cytotoxicity and synergism with copper(II) ions. The data, on the one hand, reveal that step-wise methylation of Triapine results in a change of the mode of action, which might be associated with the interaction of the intracellular copper balance. However, on the other hand, these effects do not seem to be responsible for the increased cytotoxic activity of some derivatives into the nanomolar range.

Experimental Section

tert-Butyl-(2-bromopyridin-3-yl)carbamate (**1**), *tert*-butyl (2-formylpyridin-3-yl)carbamate (**2**), Triapine and H_2NNMe_2 were synthesized as previously reported²³. All other solvents and chemicals were purchased from commercial suppliers and used without further purification. Elemental analyses were performed by the Microanalytical Laboratory of the University of Vienna and are within $\pm 0.4\%$, confirming $>95\%$ purity. All chromatographic separations were performed on silica gel. UV/vis spectra were recorded on an Agilent 8453 spectrophotometer from 200 to 1000 nm in PBS buffer pH 7.4 ($<0.5\%$ DMSO). ESI-MS spectrometry was carried out with a Bruker Esquire₃₀₀₀ ion trap spectrometer (Bruker Daltonics, Bremen, Germany). Expected and experimental isotope distributions were compared. ^1H and ^{13}C one- and two-dimensional NMR spectra were recorded in $\text{DMSO-}d_6$, with a Bruker Avance III 500 MHz FT-NMR spectrometer at 500.10 (^1H) and 125.75 (^{13}C) MHz at 298 K. The residual ^1H and ^{13}C present in $\text{DMSO-}d_6$ were used as internal references. Abbreviations for NMR data: py =

pyridine, C_q, py = quaternary carbon of pyridine. The fast relaxation of the HCl salts **MeHNNH₂** and **MeHNNHMe** prevented the exact assignment of all protons and the detection of all carbon signals. Fluorescence measurements were performed on a Horiba FluoroMax[®]-4 spectrofluorometer and processed using the FluorEssence v3.5 software package. All tested solutions had a concentration of 1×10⁻⁵ M. Scans were run at room temperature in 1% DMSO/PBS pH 7.4 with excitation and emission slit widths of 4 nm.

Synthesis

3-aminopyridine-2-carbaldehyde N-methylthiosemicarbazone (H₂NNHMe). *tert*-Butyl (2-formylpyridin-3-yl)carbamate (**2**) (147 mg, 0.66 mmol) was dissolved in EtOH (3 mL)/H₂O (1 mL) and 4-methylthiosemicarbazide (70 mg, 0.59 mmol) as well as conc. HCl (0.3 mL) were added. The reaction mixture was refluxed for 3 h and cooled to RT. The precipitate was filtered, washed with EtOH and dried *in vacuo*. **H₂NNHMe·HCl** was dissolved in water at 70 °C and 10% aq. NaHCO₃ (0.8 mL) was added. After 1 h the precipitate was filtered off, washed with cold EtOH and Et₂O and dried *in vacuo*. Yield: 110 mg (89%). Anal. Calcd. for C₈H₁₁N₅S (*M_r* 209.27 g/mol): C, 45.91; H, 5.30; N, 33.47; S, 15.32. Found: C, 45.57; H, 5.47; N, 33.27; S, 15.12. UV/vis (PBS), λ_{max}, nm (ε, M⁻¹ cm⁻¹): 259 (17800), 284 (17470), 359 (23750). ESI-MS in MeOH (negative): *m/z* 210 [M+H]⁺. ¹H NMR (DMSO-*d*₆): δ 11.35 (s, 1H, N-NH), 8.35–8.29 (m, 2H, HC=N and NHCH₃), 7.84 (dd, ³*J* = 4 Hz, ⁴*J* = 1 Hz, 1H, H_{py}), 7.16 (dd, ³*J* = 8 Hz, ⁴*J* = 1 Hz, 1H, H_{py}), 7.08 (dd, ³*J* = 8 Hz, ³*J* = 4 Hz, 1H, H_{py}), 6.46 (s, 2H, NH₂), 3.03 (d, ³*J* = 4 Hz, 3H, NHCH₃) ppm. ¹³C NMR (DMSO-*d*₆): δ = 177.6 (C=S), 149.3 (C=N), 144.3 (C_q, py), 137.7 (C_{py}), 133.5 (C_q, py), 124.8 (C_{py}), 122.7 (C_{py}), 31.7 (CH₃) ppm.

tert-Butyl (2-bromopyridin-3-yl)(methyl)carbamate (3). *tert*-Butyl-(2-bromopyridin-3-yl)carbamate (**1**) (1.0 g; 3.66 mmol) was dissolved in dry DMF (20 mL) at 0 °C and 60% NaH in mineral oil (183 mg, 4.58 mmol) was slowly added. The solution was stirred for 20 min and MeI (0.26 mL, 4.18 mmol) was added drop-wise. After 30 min at 0 °C the solution was additionally stirred for 1 h at RT. The reaction was quenched with water (20 mL) and the solvents were evaporated under reduced pressure. The residue was dissolved in water and extracted with Et₂O. The organic layers were washed with H₂O, 0.1 M HCl, sat. NaHCO₃ solution and brine, dried over Na₂SO₄, evaporated under reduced pressure and dried *in vacuo*. *n*-Hexane was added to precipitate the product. The product was used without further purification. Yield: 0.84 g (85%). ¹H NMR (DMSO-*d*₆): δ 8.37–8.30 (m, 1H, H_{py}), 7.90 (dd, ³*J* = 8 Hz, ⁴*J* = 2 Hz, 1H, H_{py}), 7.51 (dd, ³*J* = 5 Hz, ³*J* = 8 Hz, 1H, H_{py}), 3.11 and 3.08 (s, 3H, NCH₃), 1.48 and 1.30 (s, 9H, (CH₃)₃) ppm.

tert-Butyl (2-formylpyridin-3-yl)(methyl)carbamate (4). Compound **3** (1.0 g; 3.48 mmol) was dissolved in dry THF (15 mL) at –78 °C and *n*-BuLi (2.6 mL, 4.18 mmol) was slowly added. After 1 h, DMF (0.31 mL, 4.18 mmol) was added and the reaction mixture was allowed to slowly warm up to RT. Subsequently, after addition of 1.5 M HCl (1.5 mL) the pH was adjusted to about 7 with Na₂CO₃. The solution was extracted with EtOAc (3x), H₂O (2x) and brine (1x), dried over Na₂SO₄, evaporated under reduced pressure and dried *in vacuo*. Yield: 0.69 g (82%). ¹H NMR (DMSO-*d*₆): δ 10.01 (br. s, 1H, CHO), 8.70 (dd, ³*J* = 5 Hz, ⁴*J* = 1 Hz, 1H, H_{py}), 7.94 (dd, ³*J* = 8 Hz, ⁴*J* = 1 Hz, 1H, H_{py}), 7.73 (dd, ³*J* = 8 Hz, ³*J* = 5 Hz, 1H, H_{py}), 3.15 (br. s, 3H, NCH₃), 1.46 and 1.23 (s, 9H, (CH₃)₃) ppm.

3-(methylamino)pyridine-2-carbaldehyde thiosemicarbazone hydrochlorid (MeHNNH₂).

The synthesis of MeHNNH₂ was already reported in literature, but using a different synthetic strategy⁴². Compound **4** (100 mg, 0.42 mmol) was dissolved in EtOH (3.5 mL)/H₂O (0.65 mL) and thiosemicarbazide (42.4 mg, 0.47 mmol) as well as conc. HCl (176 μL) were added. The red solution was refluxed for 4 h and cooled to RT. The orange precipitate was isolated by filtration, washed with cold EtOH and dried *in vacuo*. Yield: 81 mg (78%). Anal. Calcd. for C₈H₁₁N₅S·HCl (*M_r* = 245.73 g/mol): C, 39.10; H, 4.92; N, 28.50. Found: C, 39.10; H, 5.00; N, 28.23. ESI-MS in MeOH (negative): *m/z* 208 [M-HCl-H]⁻. UV/vis (PBS), λ_{max}, nm (ε, M⁻¹ cm⁻¹): 263 (10690), 291 (11620), 383 (11370). ¹H NMR (DMSO-*d*₆): δ 11.84 (s, 1H, NH), 8.51 (s, 1H), 8.41 (s, 2H), 8.02 (d, ³*J* = 8 Hz, 1H), 7.58 (br. s, 2H), 7.27 (v. br. s, 1H), 2.94 (s, 3H, NCH₃) ppm. ¹³C NMR (DMSO-*d*₆): δ = 178.6 (C=S), 145.8 (C_q, py), 129.0 (C_{q,py}), 126.7 (C_{py}), 124.5 (C_{py}), 30.3 (NHCH₃) ppm (due to the fast relaxation of the HCl salt not all of the ¹³C signals could be observed).

3-(methylamino)pyridine-2-carbaldehyde N-methylthiosemicarbazone hydrochlorid (MeHNNHMe).

Compound **4** (98.7 mg, 0.418 mmol) was dissolved in EtOH (1.15 mL)/H₂O (0.55 mL) and 4-methylthiosemicarbazide (34.8 mg, 0.46 mmol) as well as conc. HCl (0.15 mL) were added. The solution was refluxed for 3 h and cooled to RT. The orange precipitate was separated by filtration, washed with cold EtOH and dried *in vacuo*. Yield: 87 mg (80%). Anal. Calcd. for C₉H₁₃N₅S·HCl (*M_r* = 223.30 g/mol): C, 41.61; H, 5.43; N, 26.96. Found: C, 41.59; H, 5.43; N, 26.89. ESI-MS in MeOH (negative): *m/z* 222 [M-HCl-H]⁻. UV/vis (PBS), λ_{max}, nm (ε, M⁻¹ cm⁻¹): 267 (15323), 286 (15334), 383 (14583). ¹H NMR (DMSO-*d*₆): δ 12.01 (s, 1H, N-NH), 9.01 (s, 1H, NH), 8.38 (s, 1H, HC=N), 8.03 (dd, ³*J* = 5 Hz, ⁴*J* = 2 Hz, 1H, H_{py}), 7.66 – 7.57 (m, 2H, H_{py}), 7.39 (v. br. s., 1H, NH), 3.06 (d, 3H, ³*J* = 5 Hz, S=CNHCH₃), 2.95 (s, 3H,

$C_{\text{qpy}}\text{NHCH}_3$) ppm. ^{13}C NMR (DMSO- d_6): $\delta = 178.3$ (C=S), 145.7 ($C_{\text{q, py}}$), 129.4 (C_{py}), 126.5 (C_{py}), 122.9 ($C_{\text{q, py}}$), 31.6 (S=CNHCH₃), 30.3 ($C_{\text{py}}\text{NHCH}_3$) ppm (due to the fast relaxation of the HCl salt not all of the ^{13}C signals could be observed).

3-(methylamino)pyridine-2-carbaldehyde *N,N*-dimethylthiosemicarbazone hydrochlorid (MeHNMe₂). Compound **4** (100 mg, 0.42 mmol) was dissolved in EtOH (1.15 mL)/H₂O (0.55 mL) and 4,4-dimethyl-3-thiosemicarbazide (50 mg, 0.42 mmol) as well as conc. HCl (133 μL) were added. The solution was refluxed for 4 h and stored at 4 °C overnight. The brown precipitate was separated by filtration, washed with cold isopropanol and dried *in vacuo*. Yield: 62 mg (54%). Anal. Calcd. for C₁₀H₁₅N₅S·HCl ($M_r = 273.73$ g/mol): C, 43.87; H, 5.89; N, 25.58; S, 11.71. Found: C, 43.85; H, 5.92; N, 25.36; S, 11.75. ESI-MS in MeOH (negative): m/z 236 [M-HCl-H]⁻. UV/vis (PBS), λ_{max} , nm (ϵ , M⁻¹ cm⁻¹): 264 (22980), 288 (13530), 384 (14860). ^1H NMR (DMSO- d_6): δ 12.15 (s, 1H, N-NH), 9.55 (br. s, 1H, NHCH₃), 8.96 (s, 1H, HC=N), 8.02 (dd, $^3J = 4$ Hz, $^4J = 2$ Hz, 1H, H_{py}), 7.73 – 7.65 (m, 2H, H_{py}), 3.37 (s, 6H, N(CH₃)₂), 3.04 (s, 3H, NHCH₃) ppm. ^{13}C NMR (DMSO- d_6): $\delta = 180.2$ (C=S), 145.3 ($C_{\text{q, py}}$), 138.8 (C=N), 128.5 ($C_{\text{q, py}}$), 128.2 (C_{py}), 126.0 (C_{py}), 124.2 (C_{py}), 41.7 (N(CH₃)₂), 30.3 (NCH₃) ppm.

2-bromo-*N,N*-dimethylpyridin-3-amine (5). 3-Amino-2-bromopyridine (1.5 g, 8.67 mmol) was dissolved in dry DMF (30 mL) at 0°C and 60% NaH (956 mg, 23.9 mmol) was slowly added. The solution was stirred for 20 min and MeI (1.24 mL, 19.94 mmol) was added drop-wise. After 30 min at 0 °C and 1 h at RT the reaction was quenched with water (3 mL). The solvents were evaporated under reduced pressure, the residue dissolved in water and extracted with Et₂O. The organic layer was washed with H₂O, 0.1 M HCl, sat. NaHCO₃ solution and brine, dried over Na₂SO₄, evaporated under reduced pressure and dried *in vacuo*. The mineral oil was removed by

column chromatography (pure *n*-hexane and subsequently pure ethyl acetate to elute the product).

Yield: 1.24 g (71%). ¹H NMR (DMSO-*d*₆): δ 8.01 (dd, ³*J* = 5 Hz, ⁴*J* = 2 Hz, 1H, H_{py}), 7.56 (dd, ³*J* = 8 Hz, ⁴*J* = 2 Hz, 1H, H_{py}), 7.38 (dd, ³*J* = 8 Hz, ³*J* = 5 Hz, 1H, H_{py}), 2.76 (s, 6H, NCH₃) ppm.

3-(dimethylamino)picolinaldehyde (6). Compound **5** (600 mg; 2.98 mmol) was dissolved in dry THF (12 mL), cooled to -78°C and *n*-BuLi (3.8 mL, 5.96 mmol) was slowly added. After 1 h DMF (0.3 mL, 3.87 mmol) was added and the reaction mixture was allowed to slowly warm up to RT. Subsequently, 1 M HCl (2 mL) was added and the pH adjusted to about 7 with Na₂CO₃. The product was extracted with EtOAc (3x) and washed with H₂O (2x) and brine (1x), dried over Na₂SO₄, evaporated under reduced pressure and dried *in vacuo*. Purification was performed *via* column chromatography (EtOAc:hexane, 6:1) Yield: 0.24 g (54%). ¹H NMR (DMSO-*d*₆): δ 9.93 (d, *J* = 1 Hz, 1H, CHO), 8.20 (dd, ³*J* = 4 Hz, ⁴*J* = 1 Hz, 1H, H_{py}), 7.53 – 7.50 (m, 1H, H_{py}), 7.46 (dd, ³*J* = 9 Hz, ³*J* = 4 Hz, 1H, H_{py}), 2.91 (s, 6H, NCH₃) ppm.

3-(dimethylamino)pyridine-2-carbaldehyde thiosemicarbazone (Me₂NNH₂). Compound **6** (150 mg, 1.00 mmol) was dissolved in EtOH (2 mL)/H₂O (1 mL) and thiosemicarbazide (91 mg, 1.00 mmol) was added. The reaction mixture was refluxed for 3 h, cooled to RT and the solvent was removed under reduced pressure. Purification was performed *via* column chromatography. Pure ACN was used until the first impurity had been eluted and afterwards ACN:MeOH (9:1). Yield: 94 mg (42%). Anal. Calcd. for C₉H₁₃N₅S (*M*_r = 223.30 g/mol): C, 48.41; H, 5.87; N, 31.36; S, 14.36. Found: C, 48.32; H, 5.89; N, 31.16; S, 14.25. ESI-MS in MeOH (positive): *m/z* 246 [M+Na]⁺. UV/vis (PBS), λ_{max}, nm (ε, M⁻¹ cm⁻¹): 292 (14190), 348 (9530). ¹H NMR (DMSO-*d*₆): *E isomer* δ 11.59 (s, 1H, NH), 8.41 (s, 1H, HC=N), 8.26 (s, 1H, NH₂), 8.23 (dd, ³*J* = 5 Hz, ⁴*J* = 1 Hz, 1H, H_{py}), 7.52 (dd, ³*J* = 8 Hz, ⁴*J* = 1 Hz, 1H, H_{py}), 7.50 (s, 1H, NH₂), 7.33 (dd,

$^3J = 8$ Hz, $^3J = 5$ Hz, 1H, H_{py}), 2.74 (s, 6H, $N(CH_3)_2$). ^{13}C NMR (DMSO- d_6): *E isomer* $\delta = 178.8$ (C=S), 149.9 ($C_{q, py}$), 144.4 ($C_{q, py}$), 142.8 (C_{py}), 141.9 (C=N), 126.3 (C_{py}), 124.8 (C_{py}), 44.7 ($N(CH_3)_2$) ppm.

Synthesis of the pure *Z* isomer: 20 mg of the pure *E* isomer were dissolved in 20 mL acetonitrile and stirred at 37°C for 24 h. After removal of the solvent, pure *Z* isomer was isolated after column chromatography with 100% acetonitrile as eluent.

1H NMR (DMSO- d_6): *Z isomer* δ 13.92 (s, 1H, NH), 8.53 (s, 1H, NH_2), 8.35 (dd, $^3J = 5$ Hz, $^4J = 1$ Hz, 1H, H_{py}), 8.18 (s, 1H, NH_2), 7.71 (dd, $^3J = 8$ Hz, $^4J = 1$ Hz, 1H, H_{py}), 7.49 (s, 1H, HC=N), 7.47 (dd, $^3J = 8$ Hz, $^3J = 5$ Hz, 1H, H_{py}), 2.82 (s, 6H, $N(CH_3)_2$) ppm. ^{13}C NMR (DMSO- d_6): *Z isomer* $\delta = 179.3$ (C=S), 150.4 ($C_{q, py}$), 144.2 ($C_{q, py}$), 141.4 (C_{py}), 131.2 (C=N), 128.0 (C_{py}), 125.6 (C_{py}), 45.0 ($N(CH_3)_2$) ppm.

3-(dimethylamino)pyridine-2-carbaldehyde *N*-methylthiosemicarbazone (Me₂NNHMe).

Compound **6** (70 mg, 0.47 mmol) was dissolved in EtOH (2 mL) and 4-methylthiosemicarbazide (49.5 mg, 0.47 mmol) was added. The solution was stirred for 1 h at RT and 4 h at 50°C. Subsequently, the solvent was evaporated under reduced pressure. Purification was performed *via* column chromatography using ACN/ $CHCl_3$ (10:1) and ACN/MeOH (95:5) for final elution of the product. Yield: 93 mg (83%). Anal. Calcd. for $C_{10}H_{15}N_5S$ (M_r 237.32 g/mol): C, 50.61; H, 6.37; N, 29.51; S, 13.51. Found: C, 50.57; H, 6.39; N, 29.23; S, 13.51. ESI-MS in MeOH (negative): m/z 236 $[M-H]^-$. UV/vis (PBS), λ_{max} , nm (ϵ , $M^{-1} cm^{-1}$): 290 (26410), 348 (19380). 1H NMR (DMSO- d_6): *E isomer* δ 11.60 (s, 1H, N-NH), 8.42 (s, 1H, HC=N), 8.25 (dd, $^3J = 4$ Hz, $^4J = 1$ Hz, 1H, H_{py}), 8.20 – 8.16 (m, 1H, $NHCH_3$), 7.52 (dd, $^3J = 8$ Hz, $^4J = 1$ Hz, 1H, H_{py}), 7.33 (dd, $^3J = 8$ Hz, $^3J = 4$ Hz, 1H, H_{py}), 3.04 (d, $^3J = 5$ Hz, 3H, $NHCH_3$), 2.74 (s, 6H, $N(CH_3)_2$). ^{13}C NMR

(DMSO-*d*₆): *E* isomer δ = 178.5 (C=S), 150.0 (C_{q, py}), 144.8 (C_{q, py}), 142.9 (C_{py}), 141.1 (C=N), 126.2 (C_{py}), 124.7 (C_{py}), 44.8 (N(CH₃)₂), 31.4 (CH₃) ppm.

Synthesis of the *Z* isomer: 20 mg of the pure *E* isomer were dissolved in 8 mL acetonitrile and stirred at 37°C for 24 h. After removal of the solvent, pure *Z* isomer was isolated after column chromatography using 100% acetonitrile and for final elution acetonitrile/MeOH (95:5). ¹H NMR (DMSO-*d*₆): *Z* isomer δ 13.97 (s, 1H, N-NH), 8.86 (m, 1H, NHCH₃), 8.34 (dd, ³*J* = 5 Hz, ⁴*J* = 1 Hz, 1H, H_{py}), 7.71 (dd, ³*J* = 4 Hz, ⁴*J* = 1 Hz, 1H, H_{py}), 7.47 (s, 1H, HC=N), 7.46 (dd, ³*J* = 8 Hz, ⁴*J* = 5 Hz, 1H, H_{py}), 3.02 (d, ³*J* = 5 Hz, 3H, NHCH₃), 2.81 (s, 6H, N(CH₃)₂) ppm. ¹³C NMR (DMSO-*d*₆): *Z* isomer δ = 178.7 (C=S), 150.3 (C_{q, py}), 144.3 (C_{q, py}), 141.3 (C_{py}), 130.8 (C=N), 127.8 (C_{py}), 125.5 (C_{py}), 45.0 (N(CH₃)₂), 31.5 (CH₃) ppm.

3-(dimethylamino)pyridine-2-carbaldehyde *N,N*-dimethylthiosemicarbazone (Me₂NNMe₂).

Compound **6** (107 mg, 0.71 mmol) was dissolved in EtOH (3 mL) and 4,4-dimethyl-3-thiosemicarbazide (85 mg, 0.71 mmol) was added. The solution was stirred at RT for 1 h, at 50°C for 4 h and subsequently the solvent was evaporated under reduced pressure. Purification was performed *via* column chromatography using EtOAc/Hexane (9:1) and EtOAc/MeOH (95:5) for final elution of the product. Finally, the product was stirred in diethylether (2 mL) at 35°C for 3 h, the solid was filtered off and dried *in vacuo*. Yield: 60 mg (34%). Anal. Calcd. for C₁₁H₁₇N₅S (*M_r* 251.35 g/mol): C, 52.56; H, 6.82; N, 27.86; S, 12.76. Found: C, 50.58; H, 6.77; N, 27.68; S, 12.54. ESI-MS in MeOH (positive): *m/z* 252 [M+H]⁺. UV/vis (PBS), λ_{max} , nm (ϵ , M⁻¹ cm⁻¹): 280 (19380), 352 (11750). ¹H NMR (DMSO-*d*₆): *E* isomer: 11.05 (s, 1H, NH), 8.49 (s, 1H, HC=N), 8.25 – 8.22 (m, 1H, H_{py}), 7.51 (dd, ³*J* = 8 Hz, ⁴*J* = 1 Hz, 1H, H_{py}), 7.30 (dd, ³*J* = 8 Hz, ³*J* = 4 Hz, 1H, H_{py}), 3.31 (s, 6H, S=CN(CH₃)₂), 2.75 (s, 6H, C_{py}N(CH₃)₂). *Z* isomer δ 15.23 (s, 1H, NH), 8.35 (dd, ³*J* = 5 Hz, ⁴*J* = 1 Hz, 1H, H_{py}), 7.72 (dd, ³*J* = 8 Hz, ⁴*J* = 1 Hz, 1H, H_{py}), 7.71 (s, 1H,

HC=N), 7.46 (dd, $^3J = 8$ Hz, $^3J = 5$ Hz, 1H, H_{py}), 3.36 (s, 6H, S=CN(CH₃)₂), 2.83 (s, 6H, C_{py}N(CH₃)₂) ppm. ¹³C NMR (DMSO-*d*₆): *E isomer*: δ 181.2 (C=S), 149.5 (C_{q, py}), 145.2 (C_{q, py}), 143.0 (C_{py}), 142.8 (C=N), 126.2 (C_{py}), 124.4 (C_{py}), 44.8 (C_{py}N(CH₃)₂), 42.7 (S=CN(CH₃)₂). *Z isomer* δ 180.6 (C=S), 149.9 (C_{q, py}), 144.3 (C_{q, py}), 140.1 (C_{py}), 133.6 (C=N), 127.9 (C_{py}), 125.2 (C_{py}), 45.0 (C_{py}N(CH₃)₂), 41.3 (S=CN(CH₃)₂) ppm.

Crystallographic Structure Determination. X-ray diffraction measurements were performed on a Bruker D8 VENTURE system equipped with a multilayer monochromator and a Mo K/α INCOATEC microfocus sealed tube ($\lambda = 0.71073$ Å). A single crystal of approximate dimensions 0.30 mm x 0.20 mm x 0.10 mm, was coated with Paratone-N oil, mounted at room temperature on a Hampton Research 0.3-0.4 mm CryoLoop and cooled to 100 K under a stream of N₂ maintained by a KRYOFLEXI low-temperature apparatus. The crystal was positioned at 35 mm from the detector and 775 frames were collected, each for 10 s over 1° scan width. The data were processed using SAINT software⁴³. The structures were solved by direct methods and refined by full-matrix least-squares techniques. Data were corrected for absorption effects using the multi-scan method (SADABS⁴⁴). Non-hydrogen atoms were refined with anisotropic displacement parameters. Hydrogen atoms were placed at calculated positions and refined as riding atoms in the subsequent least squares model refinements. The isotropic thermal parameters were estimated to be 1.2 respectively 1.5 times the values of the equivalent isotropic thermal parameters of the atoms to which hydrogens were bound. The following computer programs were used: structure solution SHELXS-97⁴⁵; refinement SHELXL-Version 2013/3⁴⁵, OLEX2⁴⁶; molecular diagrams ORTEP⁴⁷; Processor: Intel Xeon CPU E3-1270 V2 @ 3.50GHz; scattering factors⁴⁸.

Crystal data for Me_2NNH_2 : $\text{C}_9\text{H}_{13}\text{N}_5\text{S}$, $M_r = 223.30$, monoclinic, $P2_1/c$, $a [\text{Å}] = 11.8688(4)$, $b [\text{Å}] = 7.6283(3)$, $c [\text{Å}] = 13.1597(5)$, $\beta = 115.668(2)$, $V = 1073.89(7) \text{ Å}^3$, $Z = 4$, $\rho_{\text{calcd}} = 1.381 \text{ g/cm}^3$, $\mu = 0.276 \text{ mm}^{-1}$, $\lambda(\text{Mo-K}\alpha) = 0.71073 \text{ Å}$, $T = 100 \text{ K}$, $2\theta_{\text{max}} = 60.27^\circ$, 17994 reflections measured, 3162 unique ($R_{\text{int}} = 0.0413$), $R_1 = 0.0354$, $wR_2 = 0.0931$, GOF = 1.046. Crystallographic data have been deposited at the Cambridge Crystallographic Data Center with number CCDC1449031.

Interconversion studies of the isomers by HPLC-MS. Sample preparation: DMSO stock solutions of the compounds were diluted with PBS (pH 7.4) to a final concentration of 50 μM (1% DMSO), followed by immediate LC-MS measurements. **LC-MS system:** The chromatographic separation was performed with an Atlantis T3 C18 reversed-phase column (150 mm \times 2.1 mm, 3 μm particle size) from Waters (Milford, USA). As a mobile phase a gradient prepared from water containing 1 % (v/v) acetonitrile and 0.1 % (v/v) formic acid (eluent A) and acetonitrile containing 1 % (v/v) water and 0.1 % (v/v) formic acid (eluent B) was used. The mobile phase was kept constant at 10 % B for 1 min. Then, B was increased to 50 % within 5 min and kept for 2 min. Subsequently, B was increased to 90 % within 0.1 min and kept for 0.9 min to flush the column, followed by reconstitution of the starting conditions within 0.1 min and re-equilibration with 10 % B for 8.9 min (total analysis time = 18 min). Due to the high affinity of thiosemicarbazones for metal ions even within a HPLC system, the measurements were carried out on an inert HPLC system (1260 Infinity Bio-inert Quaternary LC System, Agilent Technologies), controlled by an Agilent OpenLAB CDS ChemStation Edition Rev. C.01.06[61] software, coupled to an Amazon L electrospray ionization ion trap mass spectrometry system (Bruker Daltonics). The LC-MS runs were performed in positive ionization mode with the following optimized parameters: flow rate 0.2 mL/min, injection volume 5 μL , column temperature 25 $^\circ\text{C}$ and autosampler temperature 5 $^\circ\text{C}$, drying gas 10 L/min (350 $^\circ\text{C}$), nebulizer

pressure 35 psi and capillary voltage 4000 V. The HyStar 3.2 and Data Analysis 4.0 software package (Bruker Daltonics) were used for instrument control and data processing.

Determination of the distribution coefficients ($D_{7.4}$). $D_{7.4}$ values of all compounds were determined by the traditional shake-flask method in n-octanol/buffered aqueous solution at pH 7.4 at 25 ± 0.2 °C as described previously³⁰. Two parallel experiments were performed for each sample. The compounds were dissolved at 30–45 μ M in the n-octanol pre-saturated aqueous solution of the buffer (10 mM HEPES) at constant ionic strength (0.10 M KCl). The aqueous solutions and n-octanol with 1:1 phase ratio were gently mixed with 360° vertical rotation for 3 h to avoid emulsion formation and the mixtures were centrifuged at 5000 rpm for 5 min by a temperature controlled centrifuge (Sanyo) at 25 °C. Estimated logP values of the neutral forms of the compounds were calculated using ChemDraw Ultra program (Version 10.0, 1986-2005 Cambridge Soft.).

Cell lines and culture conditions. The following human cancer cell lines were used in this study: the colon carcinoma-derived cell line SW480 and lung fibroblasts WI-38 (obtained from the American Tissue Culture Collection), the ovarian carcinoma-derived cell line A2780 (obtained from Sigma-Aldrich), the acute promyelocytic leukemia-derived cell line HL-60 (obtained from Dr. M. Center, Kansas State University), the cervix carcinoma-derived cell line KB-3-1 and the colchicine resistant subline KB-C-1 (obtained from Dr. D. W. Shen, Bethesda, Maryland). SW480 and WI-38 cells were grown in MEM with 10% FCS and A2780, KB-3-1, KB-C-1 and HL-60 cells were cultured in RPMI 1640 supplemented with 10% FCS. SW480/Tria cells were generated by continuous exposure of SW480 cells to increasing concentrations of Triapine (starting point 0.05 μ M; end point 20 μ M) over a period of one year¹⁹. Triapine was

administered to the cells once every other week at the day after passage, when cells had attached to the culture flasks.

Synergism is expressed by the combination index (CI) according to Chou and Talalay⁴⁹ using CalcuSyn software (Biosoft, Ferguson, MO, USA). CI < 0.9, CI = 0.9–1.2 or CI >1.2 represent synergism, additive effects and antagonism, respectively.

Cytotoxicity tests in cancer cell lines. To determine cell viability, either 2×10^4 cells/mL of SW480, SW480/Tria, WI-38, KB-3-1 and KB-C-1 or 3×10^4 cells/mL of A2780 cells were plated on 96-well plates (100 μ L/well) and allowed to recover for 24 h. Then, cells were exposed to the test drugs with the indicated concentrations for 72 h. In combination experiments the cells were pre-incubated for one hour with CuCl₂ (10 or 30 μ M). Anticancer activity was measured by the 3-(4,5-dimethylthiazol-2-yl)-2,5-diphenyltetrazolium bromide (MTT)-based vitality assay (EZ4U; Biomedica, Vienna, Austria) following the manufacturer's recommendations. Cytotoxicity was calculated using the Graph Pad Prism software (using a point-to-point function) and was expressed as IC₅₀ values calculated from full dose–response curves (drug concentrations inducing a 50% reduction of cell number in comparison to untreated control cells cultured in parallel).

Microscopy. Phase contrast images (Figure 3A) were taken at a 200 x-magnification at the Nikon eclipse Ti-e fluorescence microscope after incubation with Triapine and its derivatives (2.5 μ M) for 48 h. The magnified cells (Figure 3B) were photographed after 24 h of treatment at 400 x magnification at the Nikon eclipse Ti-e fluorescence microscope with a sCMOS pco.edge camera.

Measurement of intracellular ROS. 2',7'-Dichlorofluorescein diacetate (DCF-DA) was used to detect the production of ROS⁵⁰. DCF-DA stock solutions (33.4 mM) in DMSO were stored at

-20 °C. HL-60 cells (5×10^5 cells per sample in 500 μ L phenol-free Hanks balanced salt solution) were incubated with DCF-DA for 30 min. Subsequently, Triapine and its derivatives were added in the indicated concentrations for further 30 min. CuCl_2 was added as indicated (1, 2, 5 or 10 μ M) to the samples 15 min prior to addition of the thiosemicarbazones. After incubation, the mean fluorescence intensity was measured by flow cytometry using a FACSCalibur instrument (Becton Dickinson, Palo Alto, CA, USA). A concentration of 200 μ M H_2O_2 was used as the control.

Hoechst 33258/PI - staining. A staining of Hoechst 33258 combined with propidium iodide (PI) was used to measure the percentage of dead cells. Therefore, HL-60 cells (5×10^5 cells per sample in 500 μ L phenol-free Hanks balanced salt solution) were incubated with Hoechst/PI (1 μ g/mL / 2.5 μ g/mL) for 30 min. Subsequently, Triapine and its derivatives were added in the indicated concentrations for further 30 min. CuCl_2 was added as indicated (2, 5 or 10 μ M) to the samples 15 min prior to addition of the thiosemicarbazones. Pictures were taken at 200 x-magnification at the Nikon eclipse Ti-e fluorescence microscope and PI-positive cells were counted as percentage of Hoechst-positive cells. At least 300 cells were counted per sample.

Acknowledgements.

We thank Alexander Roller for X-ray diffraction measurement and refinement. This work was supported by the Austrian Science Fund (FWF) grant P22072-B11 (to W.B.), the Hungarian Research Foundation OTKA (PD103905) and the J. Bolyai Research Scholarship of the Hungarian Academy of Sciences. Sonja Hager was financed by the Initiative Krebsforschung (to P.H.) and Sebastian Kallus by the Mahlke geb. Obermann-Stiftung (to B. K.).

Abbreviations. ABCB1, P-glycoprotein; DCF-DA, 2',7'-Dichlorofluorescein diacetate; DFO,

desferrioxamine; dNTP, deoxynucleotide triphosphate; Dp44mT, di-2-pyridilketone 4,4-dimethyl-3-thiosemicarbazone; HEPES, 4-(2-hydroxyethyl)-1-piperazineethanesulfonic acid; MTT, 3-(4,5-dimethylthiazol-2-yl)-2,5-diphenyltetrazolium bromide; P44mT, pyridine-2-carboxaldehyde 4,4-dimethyl-3-thiosemicarbazone; PI, propidium iodide; ROS, reactive oxygen species; Triapine, 3-aminopyridine-2-carboxaldehyde thiosemicarbazone (3-AP).

Ancillary Information.

Supporting Information. Combination indices values for cytotoxicity in the presence of Cu(II); Impact of Cu(II) ions on the activity of Dp44mT.

Corresponding authors: Christian Kowol, Institute of Inorganic Chemistry, University of Vienna, Waehringer Str. 42, A-1090 Vienna, Austria. Phone: +43-1-4277-52609. Fax: +43-1-4277-52680. E-mail: christian.kowol@univie.ac.at and Petra Heffeter, Medical University of Vienna, Institute of Cancer Research, Borschkeg. 8a, A-1090 Vienna, Austria. Phone: +43-1-40160-57557. Fax: +43-1-40160-957555. E-mail: petra.heffeter@meduniwien.ac.at.

References

1. Torti, S. V.; Torti, F. M. Ironing out cancer. *Cancer Res.* **2011**, *71*, 1511-1514.
2. Yu, Y.; Wong, J.; Lovejoy, D. B.; Kalinowski, D. S.; Richardson, D. R. Chelators at the cancer coalface: desferrioxamine to Triapine and beyond. *Clin. Cancer Res.* **2006**, *12*, 6876-6883.
3. Estrov, Z.; Tawa, A.; Wang, X. H.; Dube, I. D.; Sulh, H.; Cohen, A.; Gelfand, E. W.; Freedman, M. H. In vitro and in vivo effects of deferoxamine in neonatal acute leukemia. *Blood* **1987**, *69*, 757-761.
4. Donfrancesco, A.; Deb, G.; Dominici, C.; Pileggi, D.; Castello, M. A.; Helson, L. Effects of a single course of deferoxamine in neuroblastoma patients. *Cancer Res.* **1990**, *50*, 4929-4930.
5. Selig, R. A.; White, L.; Gramacho, C.; Sterling-Levis, K.; Fraser, I. W.; Naidoo, D. Failure of iron chelators to reduce tumor growth in human neuroblastoma xenografts. *Cancer Res.* **1998**, *58*, 473-478.
6. Blatt, J. Deferoxamine in children with recurrent neuroblastoma. *Anticancer Res.* **1994**, *14*, 2109-2112.
7. Kalinowski, D. S.; Richardson, D. R. The evolution of iron chelators for the treatment of iron overload disease and cancer. *Pharmacol. Rev.* **2005**, *57*, 547-583.
8. Yu, Y.; Gutierrez, E.; Kovacevic, Z.; Saletta, F.; Obeidy, P.; Suryo Rahmanto, Y.; Richardson, D. R. Iron chelators for the treatment of cancer. *Curr. Med. Chem.* **2012**, *19*, 2689-2702.
9. Antholine, W. E.; Knight, J. M.; Petering, D. H. Inhibition of tumor cell transplantability by iron and copper complexes of 5-substituted 2-formylpyridine thiosemicarbazones. *J. Med. Chem.* **1976**, *19*, 339-341.

10. Yu, Y.; Kalinowski, D. S.; Kovacevic, Z.; Siafakas, A. R.; Jansson, P. J.; Stefani, C.; Lovejoy, D. B.; Sharpe, P. C.; Bernhardt, P. V.; Richardson, D. R. Thiosemicarbazones from the old to new: iron chelators that are more than just ribonucleotide reductase inhibitors. *J. Med. Chem.* **2009**, *52*, 5271-5294.
11. Finch, R. A.; Liu, M.; Grill, S. P.; Rose, W. C.; Loomis, R.; Vasquez, K. M.; Cheng, Y.; Sartorelli, A. C. Triapine (3-aminopyridine-2-carboxaldehyde- thiosemicarbazone): A potent inhibitor of ribonucleotide reductase activity with broad spectrum antitumor activity. *Biochem. Pharmacol.* **2000**, *59*, 983-991.
12. Aye, Y.; Long, M. J.; Stubbe, J. Mechanistic Studies of Semicarbazone Triapine targeting human ribonucleotide reductase in vitro and in mammalian cells tyrosyl radical yuenching not involving reactive oxygen species. *J. Biol. Chem.* **2012**, *287*, 35768-35778.
13. Seebacher, N. A.; Lane, D. J.; Jansson, P. J.; Richardson, D. R. Glucose modulation induces lysosome formation and increases lysosomotropic drug sequestration via the P-glycoprotein drug transporter. *J. Biol. Chem.* **2016**, *291*, 3796-3820.
14. Giles, F. J.; Fracasso, P. M.; Kantarjian, H. M.; Cortes, J. E.; Brown, R. A.; Verstovsek, S.; Alvarado, Y.; Thomas, D. A.; Faderl, S.; Garcia-Manero, G.; Wright, L. P.; Samson, T.; Cahill, A.; Lambert, P.; Plunkett, W.; Sznol, M.; DiPersio, J. F.; Gandhi, V. Phase I and pharmacodynamic study of Triapine, a novel ribonucleotide reductase inhibitor, in patients with advanced leukemia. *Leuk. Res.* **2003**, *27*, 1077-1083.
15. Karp, J. E.; Giles, F. J.; Gojo, I.; Morris, L.; Greer, J.; Johnson, B.; Thein, M.; Sznol, M.; Low, J. A phase I study of the novel ribonucleotide reductase inhibitor 3-aminopyridine-2-carboxaldehyde thiosemicarbazone (3-AP, Triapine) in combination with the nucleoside analog fludarabine for patients with refractory acute leukemias and aggressive myeloproliferative disorders. *Leuk. Res.* **2008**, *32*, 71-77.

16. Attia, S.; Kolesar, J.; Mahoney, M. R.; Pitot, H. C.; Laheru, D.; Heun, J.; Huang, W.; Eickhoff, J.; Erlichman, C.; Holen, K. D. A phase 2 consortium (P2C) trial of 3-aminopyridine-2-carboxaldehyde thiosemicarbazone (3-AP) for advanced adenocarcinoma of the pancreas. *Invest. New Drugs* **2008**, *26*, 369-379.
17. Knox, J. J.; Hotte, S. J.; Kollmannsberger, C.; Winqvist, E.; Fisher, B.; Eisenhauer, E. A. Phase II study of Triapine in patients with metastatic renal cell carcinoma: a trial of the National Cancer Institute of Canada Clinical Trials Group (NCIC IND.161). *Invest. New Drugs* **2007**, *25*, 471-477.
18. Traynor, A. M.; Lee, J. W.; Bayer, G. K.; Tate, J. M.; Thomas, S. P.; Mazurczak, M.; Graham, D. L.; Kolesar, J. M.; Schiller, J. H. A phase II trial of triapine (NSC# 663249) and gemcitabine as second line treatment of advanced non-small cell lung cancer: Eastern Cooperative Oncology Group Study 1503. *Invest. New Drugs* **2010**, *28*, 91-97.
19. Miklos, W.; Pelivan, K.; Kowol, C. R.; Pirker, C.; Dornetshuber-Fleiss, R.; Spitzwieser, M.; Englinger, B.; van Schoonhoven, S.; Cichna-Markl, M.; Koellensperger, G.; Keppler, B. K.; Berger, W.; Heffeter, P. Triapine-mediated ABCB1 induction via PKC induces widespread therapy unresponsiveness but is not underlying acquired triapine resistance. *Cancer Lett.* **2015**, *361*, 112-120.
20. Yuan, J.; Lovejoy, D. B.; Richardson, D. R. Novel di-2-pyridyl-derived iron chelators with marked and selective antitumor activity: in vitro and in vivo assessment. *Blood* **2004**, *104*, 1450-1458.
21. Whitnall, M.; Howard, J.; Ponka, P.; Richardson, D. R. A class of iron chelators with a wide spectrum of potent antitumor activity that overcomes resistance to chemotherapeutics. *Proc. Natl. Acad. Sci. U S A* **2006**, *103*, 14901-14906.

22. Richardson, D. R.; Sharpe, P. C.; Lovejoy, D. B.; Senaratne, D.; Kalinowski, D. S.; Islam, M.; Bernhardt, P. V. Dipyridyl thiosemicarbazone chelators with potent and selective antitumor activity form iron complexes with redox activity. *J. Med. Chem.* **2006**, *49*, 6510-6521.
23. Kowol, C. R.; Trondl, R.; Heffeter, P.; Arion, V. B.; Jakupec, M. A.; Roller, A.; Galanski, M.; Berger, W.; Keppler, B. K. Impact of metal coordination on cytotoxicity of 3-aminopyridine-2-carboxaldehyde thiosemicarbazone (Triapine) and novel insights into terminal dimethylation. *J. Med. Chem.* **2009**, *52*, 5032-5043.
24. Heffeter, P.; Pirker, C.; Kowol, C. R.; Herrman, G.; Dornetshuber, R.; Miklos, W.; Jungwirth, U.; Koellensperger, G.; Keppler, B. K.; Berger, W. Impact of terminal dimethylation on the resistance profile of alpha-N-heterocyclic thiosemicarbazones. *Biochem. Pharmacol.* **2012**, *83*, 1623-1633.
25. Ishiguro, K.; Lin, Z. P.; Penketh, P. G.; Shyam, K.; Zhu, R.; Baumann, R. P.; Zhu, Y. L.; Sartorelli, A. C.; Rutherford, T. J.; Ratner, E. S. Distinct mechanisms of cell-kill by triapine and its terminally dimethylated derivative Dp44mT due to a loss or gain of activity of their copper(II) complexes. *Biochem. Pharmacol.* **2014**, *91*, 312-322.
26. Jansson, P. J.; Sharpe, P. C.; Bernhardt, P. V.; Richardson, D. R. Novel thiosemicarbazones of the ApT and DpT series and their copper complexes: identification of pronounced redox activity and characterization of their antitumor activity. *J. Med. Chem.* **2010**, *53*, 5759-5769.
27. Lovejoy, D. B.; Jansson, P. J.; Brunk, U. T.; Wong, J.; Ponka, P.; Richardson, D. R. Antitumor activity of metal-chelating compound Dp44mT is mediated by formation of a redox-active copper complex that accumulates in lysosomes. *Cancer Res.* **2011**, *71*, 5871-5880.

28. Pessôa, M.; Andrade, G. F.; Paoli Monteiro, V. R.; Temperini, M. L. 2-Formylpyridinethiosemicarbazone and methyl derivatives: spectroscopic studies. *Polyhedron* **2001**, *20*, 3133-3141.
29. Kowol, C. R.; Trondl, R.; Arion, V. B.; Jakupec, M. A.; Lichtscheidl, I.; Keppler, B. K. Fluorescence properties and cellular distribution of the investigational anticancer drug triapine (3-aminopyridine-2-carboxaldehyde thiosemicarbazone) and its zinc(II) complex. *Dalton Trans.* **2010**, *39*, 704-706.
30. Enyedy, É. A.; Zsigó, É.; Nagy, N. V.; Kowol, C. R.; Roller, A.; Keppler, B. K.; Kiss, T. Complex-formation ability of salicylaldehyde thiosemicarbazone towards ZnII, CuII, FeII, FeIII and GaIII ions. *Eur. J. Inorg. Chem.* **2012**, *25*, 4036-4047.
31. Kowol, C. R.; Nagy, N. V.; Jakusch, T.; Roller, A.; Heffeter, P.; Keppler, B. K.; Enyedy, É. A. Vanadium (IV/V) complexes of Triapine and related thiosemicarbazones: synthesis, solution equilibrium and bioactivity. *J. Inorg. Biochem.* **2015**, *152*, 62-73.
32. Gutmann, V. Empirical parameters for donor and acceptor properties of solvents. *Electrochim. Acta* **1976**, *21*, 661-670.
33. Pessôa, M. M.; Andrade, G. F.; Monteiro, V. R. P.; Temperini, M. L. 2-Formylpyridinethiosemicarbazone and methyl derivatives: spectroscopic studies. *Polyhedron* **2001**, *20*, 3133-3141.
34. Jansson, P. J.; Yamagishi, T.; Arvind, A.; Seebacher, N.; Gutierrez, E.; Stacy, A.; Maleki, S.; Sharp, D.; Sahni, S.; Richardson, D. R. Di-2-pyridylketone 4, 4-dimethyl-3-thiosemicarbazone (Dp44mT) overcomes multidrug resistance by a novel mechanism involving the hijacking of lysosomal P-glycoprotein (Pgp). *J. Biol. Chem.* **2015**, *290*, 9588-9603.
35. Jansson, P. J.; Kalinowski, D. S.; Lane, D. J.; Kovacevic, Z.; Seebacher, N. A.; Fouani, L.; Sahni, S.; Merlot, A. M.; Richardson, D. R. The renaissance of polypharmacology in the

development of anti-cancer therapeutics: Inhibition of the “Triad of Death” in cancer by Di-2-pyridylketone thiosemicarbazones. *Pharmacol. Res.* **2015**, *100*, 255-260.

36. Miah, A.; Harrington, K.; Nutting, C. Triapine in clinical practice. *Eur. J. Clin. Med. Oncol.* **2010**, *2*, 1-6.

37. Lovejoy, D. B.; Sharp, D. M.; Seebacher, N.; Obeidy, P.; Prichard, T.; Stefani, C.; Basha, M. T.; Sharpe, P. C.; Jansson, P. J.; Kalinowski, D. S. Novel second-generation di-2-pyridylketone thiosemicarbazones show synergism with standard chemotherapeutics and demonstrate potent activity against lung cancer xenografts after oral and intravenous administration in vivo. *J. Med. Chem.* **2012**, *55*, 7230-7244.

38. Enyedy, E. A.; Nagy, N. V.; Zsigo, E.; Kowol, C. R.; Arion, V. B.; Keppler, B. K.; Kiss, T. Comparative solution equilibrium study of the interactions of copper(II), iron(II) and zinc(II) with Triapine (3-aminopyridine-2-carbaldehyde thiosemicarbazone) and related ligands. *Eur. J. Inorg. Chem.* **2010**, *11*, 1717-1728.

39. Moriwaki, K.; Chan, F. K. Necrosis-dependent and independent signaling of the RIP kinases in inflammation. *Cytokine Growth Factor Rev.* **2014**, *25*, 167-174.

40. Denoyer, D.; Masaldan, S.; La Fontaine, S.; Cater, M. A. Targeting copper in cancer therapy: ‘Copper That Cancer’. *Metallomics* **2015**, *7*, 1459-1476.

41. Jungwirth, U.; Kowol, C. R.; Hartinger, C.; Keppler, B. K.; Berger, W.; Heffeter, P. Anticancer activity of metal complexes: involvement of redox processes. *Antioxid. Redox Signal.* **2011**, *15*, 1085-1127.

42. Liu, M.-C.; Lin, T.-S.; Cory, J. G.; Cory, A. H.; Sartorelli, A. C. Synthesis and biological activity of 3-and 5-amino derivatives of pyridine-2-carboxaldehyde thiosemicarbazone. *J. Med. Chem.* **1996**, *39*, 2586-2593.

43. SAINT-Plus. version 8.32b; Bruker AXS Inc.: Madison, WI. **2013**.

44. *SADABS-2012/1* Bruker AXS 2013 area detector scaling and absorption correction.
45. Sheldrick, G. M. *SHELXS-97*; Program for Crystal Structure Solution; University Göttingen: Göttingen, Germany, 1997
46. Dolomanov, O. V.; Bourhis, L. J.; Gildea, R. J.; Howard, J. A.; Puschmann, H. OLEX2: a complete structure solution, refinement and analysis program. *J. Appl. Cryst.* **2009**, *42*, 339-341.
47. Johnson, G. K. *Report ORNL-5138*, Oak Ridge National Laboratory; Oak Ridge, TN 1976.
48. *International Tables for X-ray Crystallography*; Kluwer Academic Press: Dordrecht, The Netherlands, 1992; Vol. C, Tables 4.2.6.8 and 6.1.1.4.
49. Heffeter, P.; Atil, B.; Kryeziu, K.; Groza, D.; Koellensperger, G.; Korner, W.; Jungwirth, U.; Mohr, T.; Keppler, B. K.; Berger, W. The ruthenium compound KP1339 potentiates the anticancer activity of sorafenib in vitro and in vivo. *Eur. J. Cancer* **2013**, *49*, 3366-3375.
50. Gomes, A.; Fernandes, E.; Lima, J. L. Fluorescence probes used for detection of reactive oxygen species. *J. Biochem. Biophys. Methods* **2005**, *65*, 45-80.

Table of Contents graphic

Or		yes: resis	Syncretism with t_3		
